

Chapter 2

The Qinghai–Tibet Railway Geological Environment

Abstract The environmental conditions along the Qinghai–Tibet Railway are extremely harsh, the ecology fragile, and the geological conditions complex, complicating the design and construction of the railway line. Therefore, a comprehensive analysis of the various engineering geological conditions along the line is essential for studying the line scheme. In this chapter, the geographical conditions—namely the geography, climatic characteristics, soil and vegetation, wildlife, river systems, and ecological environment—along the Qinghai–Tibet Railway are discussed. Moreover, the geological environment—the topography, formation lithology, geological structure, hydrogeology, seismic and active faults, permafrost distribution, and unfavorable and unique geology—along the railway is described in detail.

Keywords Qinghai–Tibet Railway • Physical geography • Geological environment

The anoxic atmosphere, low temperature, and complex geological and engineering geological conditions, in addition to the permafrost, landslides, debris flow, earthquakes, dust storms, snowdrifts, and other geological hazards, render harsh the landscape that the Qinghai–Tibet Railway passes through. Moreover, the ecological environment along the railway line is fragile and sensitive: if the vegetation in the permafrost region is damaged, the recovery would be very slow. Thus, three major problems were encountered in the construction of the Qinghai–Tibet Railway: permafrost, alpine hypoxia, and fragile ecology.

2.1 Physical Geography

2.1.1 *Geographical Location*

Located in central Asia at an average altitude of 4500 m and spanning more than 10° latitude, the Qinghai–Tibet Plateau is the largest and highest plateau in the world and is thus known as “the Roof of the World” and “the Third Pole of the

Earth.” This $2.5 \times 10^6 \text{ km}^2$ plateau, the highest Chinese terrain, is bordered by the Hengduan Mountains on the east, the Himalayas on the south and the west, and Kunlun Mountains on the north. The plateau comprises the Xizang Autonomous Region, Qinghai Province; parts of the Xinjiang Uygur Autonomous Region, Gansu Province, Yunnan Province, Sichuan Province; and part or all of the countries of Bhutan, Nepal, India, Pakistan, Afghanistan, and Tajikistan.

Located along north latitude $29^\circ 30' - 36^\circ 25'$ and east longitude $90^\circ 30' - 94^\circ 55'$, the Qinghai–Tibet Railway passes through the hinterland of the Qinghai–Tibet Plateau, specifically through Qinghai and two of Tibet’s provinces. This line starts from Golmud city in Qinghai Province and extends 1142 km southward to Lhasa, primarily along the Qinghai–Tibet Highway and across Naij Tal, Kunlun Pass, Wudaoliang, Tuotuoheyan, Yanshiping, Tonglha Mountains, Amdo, Nagqu, Damxung, and Yambajan (Fig. 2.1).

The average altitude of the line is approximately 4380 m, with approximately 960 km of the line being 4000 m above sea level and the nearly 550 km along permafrost regions. Figure 2.2 shows the plan and profile sections of the Qinghai–Tibet Railway. With the maximum altitude of 5072 m, it is the highest and longest plateau permafrost railway in the world, and it passes through a few national and provincial nature reserves, such as the Hoh Xil Nature Reserve, Sanjiangyuan National Nature Reserve, and Chang Tang Nature Reserve.

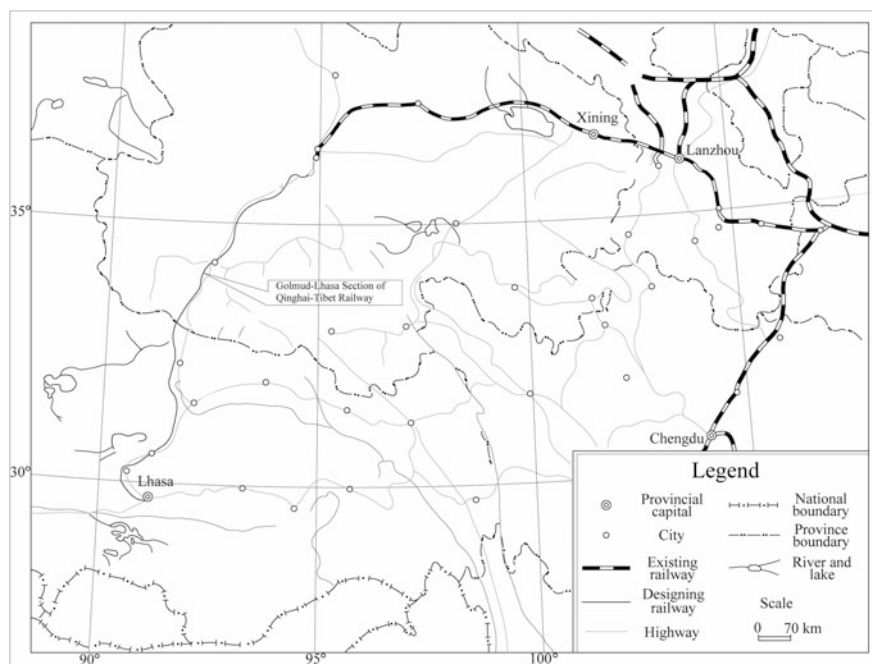


Fig. 2.1 Geographic map of the Qinghai–Tibet Railway

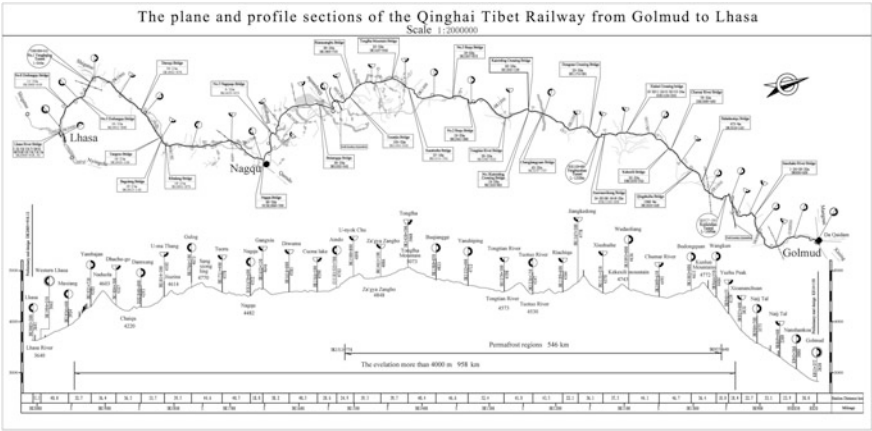


Fig. 2.2 Plane and profile sections of the Qinghai–Tibet Railway

2.1.2 Climatic Characteristics

The Qinghai–Tibet Railway is located in the Chinese mainland, far from oceans and seas. Apart from the southern Tonglha Mountains area, which has a marine climate, and the northern Qaidam area, which has an arid climate, most of the plateau hinterland has a unique climate of periglacial drought, with distinct vertical climatic zoning with increase in altitude. This region is characterized by a cold, dry, and changeable climate, without any clear seasonal distinctions; furthermore, the air rarefied, and the air pressure is low. The plateau is frozen for 7–8 months each year, typically from September to April–May, and the evaporation rate far exceeds the precipitation. In the alpine region, most of the precipitation occurs as snow, graupel, and hail; by contrast, the wide high plains see less snowfall even in winter, and rainfall accounts for 60–90% of the precipitation in the warm season. Except in certain mountain regions, snow coverage is generally unstable and thin. The prevailing winds blow toward the northwest and west, with strong winds (grade ≥ 8) mainly occurring from October to April. Table 2.1 summarizes the main meteorological conditions along the line.

The annual average temperature along the line is -6.9 to -2 $^{\circ}\text{C}$, with the highest and lowest temperatures typically occurring in July (~ 6.5 – 8.1 $^{\circ}\text{C}$) and January (occasionally, December; -17.4 to -14.5 $^{\circ}\text{C}$). The annual average temperature fluctuation is <15 – 26 $^{\circ}\text{C}$ and never exceeds 50 $^{\circ}\text{C}$. The daily average temperature fluctuation over a year is <10 – 19 $^{\circ}\text{C}$ is always less than 35 $^{\circ}\text{C}$. In contrast to the northeast permafrost region in China, the temperature characteristics in the Qinghai–Tibet Plateau vary slightly over the year but greatly within a day.

Atmospheric transparency along the line is high (low cloud, strong sunshine), and the global solar radiation and sunshine duration are high (2600 – 3000 h a^{-1}). The radiation incident on regions at altitudes below 5000 m is the highest in all of

Table 2.1 Summary of the main meteorological data along the Qinghai–Tibet Railway

Station name and construction time			Golmud (1955)		
Location and elevation			N: 36°25′	Elevation (m)	2807.6
			E: 94°54′		
Representative mileage and site			K814+150–DK957+640		
Values and data collection period			Values	Data collection period (years) and date	
Average air pressure (mb)			724.9	10	1990–1999
Temperature (°C)	Annual average		6.7	10	1990–1999
	Extreme	Maximum	35.5	45	August 2, 1999
		Minimum	−33.6	45	January 12, 1959
	Hottest monthly average		17.8	10	July
	Coldest monthly average		−8.9	10	January
	Maximum monthly averaged diurnal temperature range		19.5	10	January 1966
Humidity	Absolute (g m ^{−3})	Average	3.3	10	1990–1999
		Maximum	15	45	July 21, 1971
		Minimum	0	10	Nine times
	Relative (%)	Average	32	10	1990–1999
		Minimum	0	10	More than three times
Precipitation (mm)	Annual average		41.8	10	1990–1999
	Annual maximum		101.8	45	1967
	Annual minimum		11.4	45	1965
	Monthly maximum		44.0	45	July 1971
	Daily maximum		32.0	45	July 22, 1971
	Maximum rainfall and duration		32.0	10	13 h
	Annual average precipitation days		28.5	10	1990–1999
Evaporation (mm)	Annual average		2392.6	10	1990–1999
	Annual maximum		3232.3	45	1956
Wind speed (m s ^{−1})	Average wind speed and dominant wind direction		2.6W	10	1990–1999
	Seasonal average wind speed	Spring	3.1W	10	March–May
		Summer	2.9E	10	June–August
		Autumn	2.2W, SW	10	September–November
		Winter	2.2SW	10	December–February
	Annual average gale days (grade ≥ 8)		9.8	10	1990–1999
	Maximum wind speed and direction	Timing	24W	45	July 6, 1957
		Instantaneous	43W	10	1969

(continued)

Table 2.1 (continued)

Station name and construction time			Golmud (1955)		
Frozen snow (cm)	First and last snowfall		October 20 and May 14	45	1955–1999
	Largest maximum thickness		6.0	45	March 1985; July 1987
	Maximum seasonal frozen-soil depth and duration		88.0	45	1955–1999
Other	Annual average fog days		None	10	None
	Annual average thunderstorm days		3.3	10	1990–1999
	Annual average sandstorm days		–	–	–
Comment	Averages are calculated using data from the past 10 years; extremes are derived from the station's historical data				
Station name and construction time			Wudaoliang (October 1955)		
Location and elevation			N: 35°13'	Elevation	4612.2
			E: 93°05'	(m)	
Representative mileage and site			DK957+640–DK1160+344		
Values and data collection period			Values	Data collection period (years) and date	
Average air pressure (mb)			578.9	10	1990–1999
Temperature (°C)	Annual average		–5.2	10	1990–1999
	Extreme	Maximum	23.2	44	June 11, 1961
		Minimum	–37.3	44	January 12, 2012
	Hottest monthly average		5.6	10	1990–1999
	Coldest monthly average		16.7	10	1990–1999
	Maximum monthly averaged diurnal temperature range		18.6	44	March 1966
Humidity	Absolute (g m ^{–3})	Average	2.8	10	1990–1999
		Maximum	11	44	July 12, 1993
		Minimum	0	44	Three times
	Relative (%)	Average	57	10	1990–1999
		Minimum	0	44	Five times
Precipitation (mm)	Annual average		290.9	10	1990–1999
	Annual maximum		407.0	44	1989
	Annual minimum		136.3	44	1984
	Monthly maximum		133.1	44	July 1991
	Daily maximum		37.1	44	August 7, 1977
	Maximum rainfall and duration		37.1	44	21 h
	Annual average precipitation days		180.0	10	1990–1999
Evaporation (mm)	Annual average		1316.9	10	1990–1999
	Annual maximum		1531.6	44	1973

(continued)

Table 2.1 (continued)

Station name and construction time			Wudaoliang (October 1955)		
Wind speed (m s ⁻¹)	Average wind speed and dominant wind direction		4.1 W	10	1990–1999
	Seasonal average wind speed	Spring	4.8 W	10	1990–1999
		Summer	3.5 E	10	1990–1999
		Autumn	3.4 W, NE	10	1990–1999
		Winter	5.1 W	10	1990–1999
	Annual average gale days (grade ≥ 8)		130.1	10	1990–1999
	Maximum wind speed and direction	Timing	31 W	44	April 2, 1986
Instantaneous		40 W	44	More than five times	
Frozen snow (cm)	First and last snowfall		August 6 and July 27	44	1956–1999
	Largest maximum thickness		14.0	44	October 14, 1967
	Maximum seasonal frozen-soil depth and duration		No observation data		Permafrost area
Other	Annual average fog days		10.9	10	1990–1999
	Annual average thunderstorm days		36.7	10	1990–1999
	Annual average sandstorm days		–	–	–
Comment					
Station name and construction time			Tuotuo River (October 1955)		
Location and elevation			N: 34°13′	Elevation (m)	4533.1
			E: 92°26′		
Representative mileage and site			DK1160+344–DK1419+300		
Values and data collection period			Values	Data collection period (years) and date	
Average air pressure (mb)			585	10	1990–1999
Temperature (°C)	Annual average		–4	10	1990–1999
	Extreme	Maximum	24.7	44	June 29, 1988
		Minimum	–45.2	44	January 6, 1986
	H hottest monthly average		7.6	10	1990–1999
	Coldest monthly average		–16.2	10	1990–1999
	Maximum monthly averaged diurnal temperature range		21.8	10	January 1986
	Humidity	Absolute (g m ⁻³)	Average	3	10
Maximum			11.5	44	June 14, 1999
Minimum			0	44	Nine times
Relative (%)		Average	53	10	1990–1999
		Minimum	0	44	More than five times

(continued)

Table 2.1 (continued)

Station name and construction time			Tuotuo River (October 1955)		
Precipitation (mm)	Annual average		248.5	10	1990–1999
	Annual maximum		459.4	44	1985
	Annual minimum		164.2	44	1984
	Monthly maximum		174.0	44	July 1972
	Daily maximum		50.2	44	October 18, 1985
	Maximum rainfall and duration		50.2	44	24 h
	Annual average precipitation days		172.6	10	1990–1999
Evaporation (mm)	Annual average		1638.9	10	1990–1999
	Annual maximum		1945.5	44	1960
Wind speed (m s ^{−1})	Average wind speed and dominant wind direction		3.9 W	10	1990–1999
	Seasonal average wind speed	Spring	4.8 W	10	1990–1999
		Summer	3.5 NE, E	10	1990–1999
		Autumn	3.1 W	10	1990–1999
		Winter	4.3 W	10	1990–1999
	Annual average gale days (grade ≥ 8)		178	10	1990–1999
	Maximum wind speed and direction	Timing	30 W, SW	44	December 17, 1970
		Instantaneous	40 W	44	More than four times
Frozen snow (cm)	First and last snowfall		August 15 and July 28	44	1956–1999
	Largest maximum thickness		39	44	October 18, 1985
	Maximum seasonal frozen-soil depth and duration		No observation data	44	Permafrost area
Other	Annual average fog days		8.8	10	1990–1999
	Annual average thunderstorm days		47.8	10	1990–1999
	Annual average sandstorm days		–	–	–
Comment					
Station name and construction time			Amdo (November 1965)		
Location and elevation			N: 32°21′	Elevation (m)	4800
			E: 91°06′		
Representative mileage and site			DK1419+300–DK1633+500		
Values and data collection period			Values	Data collection period (years) and date	
Average air pressure (mb)			574.0	34	–
Temperature (°C)	Annual average		−2.9	34	–
	Extreme	Maximum	23.3	34	June 19, 1972
		Minimum	−36.7	34	January 17, 1968
	Hottest monthly average		7.5	34	July
	Coldest monthly average		−14.7	34	January
	Maximum monthly averaged diurnal temperature range		16.7	34	December

(continued)

Table 2.1 (continued)

Station name and construction time			Amdo (November 1965)		
Humidity	Absolute (g m ⁻³)	Average	3.1	34	–
		Maximum	12	34	February 25, 1972
		Minimum	0	34	Multiple times
	Relative (%)	Average	51	34	–
		Minimum	0	34	–
Precipitation (mm)	Annual average		428.4	34	–
	Annual maximum		604.6	34	1971
	Annual minimum		292.3	34	1972
	Monthly maximum		199.8	34	July 1970
	Daily maximum		35.0	34	July 18, 1983
	Maximum rainfall and duration		149.6	34	August 9, 1974; 19 days
	Annual average precipitation days		87.0	34	–
Evaporation (mm)	Annual average		1782.9	34	–
	Annual maximum		1941.1	34	1984
Wind speed (m s ⁻¹)	Average wind speed and dominant wind direction		4.3N, NE	34	–
	Seasonal average wind speed	Spring	5.8 W, SW	34	–
		Summer	3.6 NE	34	–
		Autumn	3.9 N, NE	34	–
		Winter	5.3 W	34	–
	Annual average gale days (grade ≥ 8)		147.1	34	–
	Maximum wind speed and direction	Timing	35 W, SW	34	February 6, 1976
Instantaneous		38 W	34	January 11, 1977	
Frozen snow (cm)	First and last snowfall		August 7 to July 27	34	1988
	Largest maximum thickness		20.0	34	October 4, 1968
	Largest seasonal frozen-soil depth and duration		350.0	34	–
Other	Annual average fog days		1.2	34	–
	Annual average thunderstorm days		74.8	34	–
	Annual average sandstorm days		–	–	–
Comment					
Station name and construction time			Nagqu (July 1954)		
Location and elevation			N: 31°29′	Elevation	4507.0
			E: 92°04′		
Representative mileage and site			DK1633+500–DK1797+300		
Values and data collection period			Values	Data collection period (years) and date	

(continued)

Table 2.1 (continued)

Station name and construction time			Nagqu (July 1954)		
Average air pressure (mb)			587.4	45	–
Temperature (°C)	Annual average		–1.3	45	–
	Extreme	Maximum	24.2	45	June 10, 1995
		Minimum	–41.2	45	January 16, 1968
	Hottest monthly average		8.0	45	July
	Coldest monthly average		–12.9	45	January
	Maximum monthly averaged diurnal temperature range		19.4	45	–
Humidity	Absolute (g m ^{–3})	Average	3.6	45	–
		Maximum	14.2	45	July 22, 1971
		Minimum	0	45	Multiple times
	Relative (%)	Average	54	45	–
		Minimum	0	45	–
Precipitation (mm)	Annual average		421.8	45	–
	Annual maximum		590.4	45	1980
	Annual minimum		307.5	45	1986
	Monthly maximum		211.2	45	August 1964
	Daily maximum		333	45	July 16, 1984
	Maximum rainfall and duration		138.7	45	Jul. 19, 1984; 13 days
	Annual average precipitation days		121	45	–
Evaporation (mm)	Annual average		1961.5	45	–
	Annual maximum		2116.8	45	1966
Wind speed (m s ^{–1})	Average wind speed and dominant wind direction		4.1 W	45	–
	Seasonal average wind speed	Spring	4.3 W, SW	45	–
		Summer	2.8 S, SW	45	–
		Autumn	2.6 W	45	–
		Winter	3.5 W	45	–
	Annual average gale days (grade \geq 8)		106	45	–
	Maximum wind speed and direction	Timing	37 SW	45	June 2, 1988
		Instantaneous	40 W	45	January 31, 1989
Frozen snow (cm)	First and last snowfall		August 29 to August 1	45	1985
	Largest maximum thickness		21	45	October 16, 1990
	Largest seasonal frozen-soil depth and duration		281	45	Multiple times in 1974

(continued)

Table 2.1 (continued)

Station name and construction time				Nagqu (July 1954)		
Other	Annual average fog days			4.8	45	—
	Annual average thunderstorm days			80.6	45	—
	Annual average sandstorm days			3.1	—	—
Comment						
Station name and construction time				Damxung (1962)		
Location and elevation				N: 30°29′	Elevation (m)	4201.1
				E: 91°06′		
Representative mileage and site				DK1797+300—DK1953+670		
Values and data collection period				Values	Data collection period (years) and date	
Average air pressure (mb)				604.4	37	—
Temperature (°C)	Annual average		1.6	37	—	
	Extreme	Maximum	26.5	37	June 8, 1996	
		Minimum	−35.9	37	January 16, 1968	
	Hottest monthly average		16.8	37	July	
	Coldest monthly average		−9.7	37	January	
	Maximum monthly averaged diurnal temperature range		18.6	37	January	
Humidity	Absolute (g m ^{−3})	Average	4.2	37	—	
		Maximum	13	37	September 2, 1989	
		Minimum	0	37	Multiple times	
	Relative (%)	Average	54	37	—	
		Minimum	0	37	Multiple times	
Precipitation (mm)	Annual average		468.1	37	—	
	Annual maximum		685.8	37	1971	
	Annual minimum		293.6	37	1972	
	Monthly maximum		253.2	37	July 1974	
	Daily maximum		50.4	37	July 23, 1975	
	Maximum rainfall and duration		164.8	37	August 10, 1998; 25 days	
	Annual average precipitation days		116.4	37	—	
Evaporation (mm)	Annual average		1866.1	37	—	
	Annual maximum		2295.5	37	1972	
Wind speed (m s ^{−1})	Average wind speed and dominant wind direction		2.4 SW	37	—	
	Seasonal average wind speed	Spring	3.0 SW	37	—	
		Summer	2.3 NE	37	—	
		Autumn	1.9 N, NE	37	—	
		Winter	2.4 SW	37	—	
	Annual average gale days (grade ≥ 8)		57.1	37	—	
	Maximum wind speed and direction	Timing	25 W, SW	37	March 6, 1993	
		Instantaneous	—	—	—	

(continued)

Table 2.1 (continued)

Station name and construction time			Damxung (1962)		
Frozen snow (cm)	First and last snowfall		September 2 to June 4	37	–
	Largest maximum thickness		14.0	37	October 4, 1966
	Largest seasonal frozen-soil depth and duration		11.3	37	October 4, 1968
Other	Annual average fog days		0.7	37	–
	Annual average thunderstorm days		74.8	37	–
	Annual average sandstorm days		–	–	–
Comment					
Station name and construction time			Lhasa (1955)		
Location and elevation			N: 29°40′	Elevation (m)	3648.70
			E: 91°08′		
Representative mileage and site			DK1953+670–DK2006+700		
Values and data collection period			Values	Data collection period (years) and date	
Average air pressure (mb)			652.2	44	–
Temperature (°C)	Annual average		7.8	45	–
	Extreme	Maximum	29.6	45	June 8, 1995
		Minimum	–16.5	45	January 17, 1968
	Hottest monthly average		14.5	45	July
	Coldest monthly average		–1.8	45	January
	Maximum monthly averaged diurnal temperature range		16.6	45	January
Humidity	Absolute (g m ^{–3})	Average	4.9	45	–
		Maximum	16.4	45	July 14, 1970
		Minimum	0	45	Multiple times
	Relative (%)	Average	45	45	–
		Minimum	0	45	Multiple times
Precipitation (mm)	Annual average		406.8	45	–
	Annual maximum		796.6	45	1962
	Annual minimum		229.6	45	1983
	Monthly maximum		313.5	45	August 1958
	Daily maximum		41.6	45	July 28, 1969
	Maximum rainfall and duration		262.1	45	July 6, 1984; 27 days
Evaporation (mm)	Annual average		1975.7	45	–
	Annual maximum		2873.1	45	1989

(continued)

Table 2.1 (continued)

Station name and construction time			Lhasa (1955)		
Wind speed (m s ⁻¹)	Average wind speed and dominant wind direction		2.0 E, SE	45	—
	Seasonal average wind speed	Spring	1.7 E	45	—
		Summer	2.4 E, SE	45	—
		Autumn	1.8 E, SE	45	—
		Winter	1.6 E, SE	45	—
	Annual average gale days (grade ≥ 8)		26	45	—
	Maximum wind speed and direction	Timing	16.3 N, NE	45	October 7, 1980
Instantaneous		32.3 SW, W	45	1974, 1976	
Frozen snow (cm)	First and last snowfall		October 7 to May 4	45	—
	Largest maximum thickness		12	45	December 11, 1981
	Largest seasonal frozen-soil depth and duration		2.6	45	January 29, 1966
Other	Annual average fog days		None	45	—
	Annual average thunderstorm days		68.1	45	—
	Annual average sandstorm days		—	—	—
Comment					

China ($\sim 600\text{--}800 \text{ kcal cm}^{-2} \text{ a}^{-1}$), and the radiation of each month is positive. Because of the strong winds across the plateau, the sensible heat flux and latent heat flux (60–80 and 20–30% per year, respectively) consume most of the surface energy. The vast majority (98.8%) of the radiation incident on regions at altitudes below 5000 m effuses into the atmosphere through turbulent exchange in the form of sense heat or latent heat. The remaining 1.2% of the radiation warms the soil and thaws the frozen ground, minimally increasing the ground-surface temperature in the process; however, the subsurface temperature remains low.

The Qinghai–Tibet Railway crosses three large natural climatic zones: the arid climatic zone north of Kunlun Mountains (e.g., Golmud), the plateau arid climatic zone between Kunlun Mountains and Tonglha Mountains, and the plateau subarid climatic zone south of Tonglha Mountains. From Kunlun Mountains to the hinterland of the Qinghai–Tibet Plateau, the altitude of the arid climatic zone rises up to 4500 m, the temperature and evaporation gradually decreases, precipitation gradually increases, the air pressure decreases to 560–580 mb, and the relative humidity increases to 49–52%; the annual average wind speed in this zone is 3.9–4.1 m s⁻¹. The plateau subarid climate tends to be relatively warm and humid, with an atmospheric pressure of 587–652 mb, relative humidity of 54%, and annual average wind speed of 2.0–4.1 m s⁻¹. Overall, the area along the line can be characterized as having an alpine semiarid to semihumid climate. Nevertheless, given the vastness of the landmass and its large elevation variation, characteristics of the mountainous areas on the plateau clearly differ from those of the high plains.

The annual average temperature in Kunlun Mountains, Hoh Xil Mountains, Fenghuo Mountain, and Tonglha Mountains is less than -6°C . From October to May, the temperature is less than 0°C . Rainfall occurs during June–September, and the annual evaporation exceeds 1300 mm. The wind is strong and changeable; in some intermontane valleys, the wind speed is lower and the wind direction changes frequently.

The annual average temperature of the high plains in the hinterland of the Qinghai–Tibet Plateau is -4.5 to -4°C . From October to April, the air temperature is less than 0°C , and the average minimum temperature is below -10°C . The annual precipitation is approximately 300 mm. The prevailing wind during September–May is from the west and that during June–August is from the north; the maximum wind speed is $30\text{--}31\text{ m s}^{-1}$ and occurs mostly during November–March.

The overall climatic characteristics of Amdo Valley in the south Tonglha Mountains region tends to be warm and humid despite its elevation of more than 4700 m above sea level. The annual average temperature here is -2.9°C , with subzero temperatures occurring mainly during October–April. The annual precipitation is 428.4 mm, more than 80% of which occurs during July–September. The annual evaporation is 1782.9 mm, and the annual average wind speed is 4.3 m s^{-1} .

In the region between the Nyainqentanglha Mountains and Damxung, Lhasa, the climate is relatively warm and humid, with an annual average temperature of 1.6°C , and annual average precipitation of 468.1 mm; the annual average temperature and precipitation in Lhasa alone is 7.8°C and 406.8 mm, respectively.

2.1.3 Soil and Vegetation

Because of the strong uplift of the Qinghai–Tibet Plateau, the soil and vegetation characteristics differ from those expected at the corresponding latitudes. The soil and vegetation in the plateau can be characterized as alpine meadow, grassland, and alpine desert landscapes. Given the cold and arid climatic conditions, the natural vegetation is short and sparse and exhibits such characteristics as drought resistance, wind resistance, and salt tolerance. Alpine meadow soil and alpine desert soil are widely distributed on the plateau; these soils have the characteristics of coarse texture, thin soil layer, slow pedogenesis, and poor development. The mountain altitudinal belt structure is clear at the outer edge of the plateau.

2.1.3.1 Soil

The Qinghai–Tibet Plateau mainly has meadow soil and alpine soil. Meadow soil develops under meadow vegetation in cold and wet conditions. Its formation is directly influenced by groundwater infiltration and is characterized by the accumulation of humus as well as the alternation of soil oxidation and reduction because

of periodic fluctuations in the groundwater level, which in turn results in the formation of a rust-colored stripe layer. Because meadow soil has relatively high moisture content, it supports lush vegetation with deep and dense roots. Furthermore, this vegetation supplies a large amount of organic content to the soil. When the soil freezes, the organic residues decompose slowly and incompletely, leading to gradual humus accumulation in the soil.

Alpine soil in the Qinghai–Tibet Plateau is mainly that soil formed in the vast windbreak-less mountain forest belt surrounding the plateau and the high mountain snow–ice zone. The alpine soil forms under the alpine bioclimate and exhibits distinct vertical distribution regularity: The upper permafrost layer is formed in the highest and coldest periglacial zone, which is closest to the snowline; the second layer comprises the meadow soil, frigid calcic soils, and frost desert soils in the high frigid zone; the third layer comprises the dark felty soils, cold calcic soils, and cold desert soils in the subfrigid zone; and the lowest layer is the gray-cinnamon soil of the temperate high land.

The soil along the railway line in Qinghai Province is mainly alpine meadow soil, which forms under a wet and cold climate and the alpine meadow vegetation. This soil exhibits distinct soddy process, clear humification, and varying degrees of leaching. This alpine soil has strong frost weathering characteristics, shows clear layering in the soil, and is unsuitable for planting. It can be further classified as alpine meadow soil, alpine steppe meadow soil, alpine shrub meadow soil, and alpine moist meadow soil.

On the Qinghai–Tibet Plateau, the soil distribution changes with the climate: From the southeast to the northwest, the climate changes as humid, subhumid, and semiarid, and the soils change as alpine meadow soil, dark felty soil–frigid calcic soil, cold calcic soil, cold desert alpine soil, and cold desert soil.

2.1.3.2 Vegetation

The plants along the Qinghai–Tibet Railway are of the Qinghai–Tibet Plateau subalpine meadow steppe type. The soil of the Qinghai–Tibet Plateau is generally poor because of the harsh topography and climate; consequently, the plateau vegetation is sparse, with meadow steppe and cushion plants forming most of the landscape. Given the vastness of the plateau and its diverse regional variations, the vegetation distribution varies across the plateau, with the vertical distribution pattern being especially evident. Desert steppe plants dominate the deserts and dry valleys, and the subalpine regions are covered by grassland and shrub plants. Meadow shrubs are common in the high mountain regions, whereas cushion plants are present near the summits, under the snowbelt. Only two types of vegetation can be found in the dry and cold desert regions, such as the Qiangtang Plateau: alpine cushion plants and alpine desert plants. The Qinghai–Tibet Plateau does not have forests, except in the southeast of the plateau (i.e., the northern section of Hengduan Mountains), where the warm and humid airflow from the ocean supports mountain coniferous forests. In the cold, wet, and humid high plains, such as the Qinghai

Plateau and Yushu Plateau, the meadow steppe serves as pastures and supports animal husbandry. The Qinghai–Tibet Plateau has two dry and cold desert regions: Qaidam Basin and Kunlun–Altun Mountains in the north and the eastern Pamirs in the west. The vegetation in the Qaidam Basin is mainly semishrub and shrub deserts, similar to the desert in Tarim Basin. The bleak desert climate of the Kunlun–Altun Mountains sees almost no vegetation. In Pamir–Karakoram, desert grasslands dominate the upper regions, where the lower regions contain alpine meadows or deserts. Because of limited rainfall, only a few Schrenk spruce trees grow in southern Yecheng. The lower regions of the Qilian Mountains have desert steppe or steppe vegetation, and in the subalpine belt, the southeast monsoon nourishes spruce forests and secondary deciduous forests and shrubs; the upper regions contain alpine grasslands and a few alpine plants. In the southern regions of the plateau, the valley between the Kailas Range and the Himalayas has a landscape of xerophytic thorn shrubs and steppe, whereas the alpine belt is dominated by alpine meadows and cushion plants.

Vegetation on the Qinghai–Tibet Plateau exhibits clear vertical zonation. In the 3000–4000 m elevation belt, the mountain area in the southeast is influenced by the southwest monsoon; this belt has a relatively humid climate, with vertical distributions of subtropical moist evergreen broad-leaved forests, mixed-wood forests, and cold temperate coniferous forests. In the 4000–4500 m elevation belt, the westerly circulation has a strong influence in the northern plateau, whereas the southwest monsoon has a weaker effect; the climate cold here supports vegetation alpine shrub grasslands and meadows. In northern Tibet, regions with an average altitude of 5000 m are mostly influenced by the westerly circulation; the climate is extremely arid and cold, and alpine desert vegetation is common. The temperate belt at 4200–4500 m elevation sees mountain temperate desert vegetation and steppe desert vegetation.

The main types of vegetation along the railway are alpine meadow, alpine shrub meadow, alpine steppe, and alpine desert steppe. In particular, semishrubs and herbs, such as Gramineae, Chenopodiaceae, Compositae, *Dasiphora fruticosa* of Rosaceae, and *Arenaria* of Caryophyllaceae, which are capable surviving in the arid climate, are common. On the basis of vegetation ecology, the area from Golmud to Lhasa can be classified as follows: Gobi bare land (Golmud to Nanshankou); mountain desert and mountain grassland (Nanshankou to Kunlun Mountains); alpine meadow, grassland, and desert (Golmud to Tonglha Mountains); alpine meadow (Tonglha Mountains to Damxung); and bushveld (Damxung to Lhasa).

Given the variation in water availability, temperature, topography, and especially altitude, the southern areas along the railway line are species-rich, whereas the high plains and the northern regions have successively fewer vegetation species. Table 2.2 lists the vegetation ecological areas along the line.

There are 305 species and varieties (22 shrubs, 283 herbs) of seed plants, belonging to 40 families and 134 genera, in the area along the railway. Around 40 species, including four shrubs, are dominant, examples of which include *Stipa purpurea*, *Festuca rubra*, *Elymus nutans*, *Orinus*, *Kobresia humilis*, *Himalayan Kobresia humilis*, *Carex moocroftii*, and *Edelweiss*.

Table 2.2 Ecological regionalization of the Qinghai–Tibet Railway

No.	Location	Ecological regionalization	Dominant vegetation
1	Nanshankou to Naij Tal	Desert	Xerophilous shrub
2	Dongxidatan to Fenghuo Mountain Pass	Alpine steppe	Carexmoorcroftii, Compositae, Gramineae
3	Wuli to Amdo	Secondary alpine steppe	Compositae, Gramineae, Cyperus
4	North Tonglha Mountains to Wumatang	Alpine meadow	Kobresia pygmaea
5	Damxung area	Meadow–grassland transition	Kobresia Cyperus
6	Yangbaling to Lhasa	Shrub grassland	Potentilla

East of eastern Nyainqentanglha mountains, the rivers are parallel and the relief great; this region is strongly influenced by the southwest monsoons and the southeast monsoons, which bring substantial rainfall. Consequently, this region has tropical, subtropical, and warm temperate forests dominated by woody species, and the distribution of these forests exhibit clear vertical zonation. Southeastern Qinghai and northwestern Sichuan, located in the transition zone of the alpine valleys and the plateau, have a low and gentle surface relief, and the landscape is dominated by alpine shrubs (e.g., *Caragana*, *Dasiphora fruticose*, and *Salix cupularis*) and alpine meadows (e.g., grain grass (Xiaoman grass), *Kobresia humilis*, Tibetan wormwood, and *Carex*). The vegetation on the meadows is rich in nutrition and has high palatability and thus is all good pastures. Winters here are cold and dry and the summers warm and humid. West of this belt, the grass is low (e.g., *Ceratoides compacta*, *Ajania tibetica*, *Arenaria*, and *Myricaria*) and the vegetation coverage sparse, short, and monotonous, with *Stipa* L. (Gramineae), such as *Stipa bungeana*, *Stipa breviflora*, *Stipa purpurea*, *Stipa krylovii*, and *Artemisia*, being dominant.

Vegetation coverage on the Qinghai–Tibet Plateau has increased in recent years, with anthropogenic activity having little effect in this region. From 1982 to 1991, vegetation in the plateau exhibited an increasing trend, but in the southeast–northwest region, the rate of increase has gradually reduced, which is consistent with the gradually worsening climatic conditions and meridional and zonal variation from the southeast to the northwest. From 1992 to 2002, vegetation in the central and northwest plateau exhibited a decreasing trend, with areas along the Yangtze River, Yellow River, Lancang River, and the source region of Nujiang River being the worst affected; this also evidences that the climatic conditions in the middle and northwest plateau are not conducive to vegetation growth. The middle and northwest regions of the plateau are the most sensitive to climate change. Because of temperature variation, plateau vegetation changed within 7 and 3.5 years, indicating its sensitivity to temperature variation. From 1982 to 2002, seven of the eight main vegetation types in the plateau exhibited varying but overall increasing growth trends; the vegetation in the cold and arid regions however were vulnerable to climate change and were slow to recover.

2.1.4 Rare Wild Animals

More than ten types of rare wild animals, mostly mammals and birds, are distributed along the Qinghai–Tibet Railway. On the basis of their habitat, these animals can be categorized as intermountain lake basin fauna and broad valley fauna, mountain mammalian fauna, and wetland animal fauna.

1. Intermountain lake basin fauna and broad valley fauna—This type includes species endemic to the Qinghai–Tibet Plateau, such as the Tibetan antelope, *Equus kiang*, *Bos mutus*, and *Procapra picticaudata*, which are distributed in flat terrains, intermountain basins, lakeshores, and occasionally in broad river shoals. They avoid predators through aggregation and by running.
2. Mountain mammalian fauna—Animals of this type (e.g., *Pseudois nayaur*, *Ovis ammon*, White-lipped deer, lynx, snow leopard, and brown bear) prefer the mountains. The Artiodactyla animals, for example, evade predators by clustering and relying on their good climbing abilities.
3. Wetland animal fauna—This type includes wading and swimming birds (e.g., black-necked crane, bar-headed goose, red chicken, and brown-headed gull) mainly live in rivers, lakes, marshes, and swamps.

2.1.5 River System

The Qinghai–Tibet Railway passes through five major river systems: (north to south) the Qaidam Inland River System, Yangtze River, Za'gya Zangbo Inland River System, Nujiang River, and Yalu Tsangpo River. The main rivers are Golmud and Kunlun Rivers of the Qaidam Inland River System; Qingshui, Chumar, Tuotuo, Tongtian, and Buqu rivers of the Yangtze River system; Za'gya Zangbo and Rianazangbu Meanders of the Za'gya Zangbo Inland River System; Lari Meander, Beisang Meander, Liantong River, Nagqu, and Muge Meander of the Nujiang River system; and Dam Qu River, Doilung Meander, and Lhasa River of the Yalu Tsangpo River system. These rivers, all of which have a low temperature, are mainly fed by meltwater and meteoric water, and thus, exhibit seasonal variations in their water level.

The major hydrological characteristics of these rivers are as follows:

1. The Qaidam Inland River System develops north of Kunlun Mountains, and its main river is Golmud River, which is known as Kunlun River upstream. This river has a few branch ditches (e.g., Xiaonanchuan and Wanbaogou) on both its shores. The landform is of the mountains and Gobi type, and the flood level varies suddenly and widely.
2. The Yangtze River system develops in the region south of Kunlun Mountains and to northern Tonglha Mountains, and its major constituents are Chumar River, Tuotuo River, and Tongtian River. The runoff for these rivers primarily

depends on precipitation, with minor contributions from glacier-melt and snowmelt water. The landform is of the low mountains and hills type and is composed of large semiarid grasslands and swamp lakes. Hummocks, ice cones, and icy mantles form in winter. This area has the well-known Hoh Xil Nature Reserve, which contains the source of Changjiang River.

3. The Za'gya Zangbo Inland River System forms between the southern Tonglha Mountains and northern Touerjiu Mountains, and its main river is the Za'gya Zangbo Meander. Its runoff is mainly from precipitation and meltwater. The landform is of the low mountains and hills type, with sparse pastures and numerous swamps and wetlands in the valleys.
4. The Nujiang River system, which comprises Nagqu and Beisang Qu rivers, develops in the region south of Touerjiu Mountains and to northern Nyainqentanglha Mountains. The landform is of the high plains semihumid meadow type and has dense pastures and numerous marsh wetlands. The permafrost and nonpermafrost areas are north and south of Amdo, respectively.
5. The Yalu Tsangpo River system, whose major constituents include Lhasa River and its ditches (namely Doilung Meander, Dam Qu, and Xiongqu) run south of Nyainqentanglha Mountains. The upstream region of Lhasa River starts is of the low mountain meadow type, the middle and lower reaches alpine, and the valley broad.

2.1.6 Ecological Environment

The Qinghai–Tibet Plateau can be characterized as having a high altitude, thin air, a cold arid climate, a short plant-growth period, low biomass, and a simple food chain. Its ecological environment is fragile because the material recycling and energy conversion processes are slow. In addition, because of the long low-temperature periods and the short growing season, the recovery of any destroyed vegetation is very slow; this in turn accelerates the melting of frozen soil, leading to desertification and soil erosion. Therefore, the World Wide Fund for Nature has listed the Qinghai–Tibet Plateau as a top priority for global biodiversity conservation.

2.2 Topography and Geomorphology

Except for the region between Golmud and Nanshankou in the southern edge of Qaidam Basin, the Qinghai–Tibet Railway passes entirely through high plains. The main mountains along the railway are Kunlun Mountains, Hoh Xil Mountains, Fenghuo Mountain, Kaixinling, Tonglha Mountains, Touerjiu Mountains, and Nyainqentanglha Mountains. The strikes of these mountains are almost WN–ES,

and the relative elevation is mostly less than 300 m. Similar to an undulating dome, these mountains have gentle slopes, narrow bodies, and broad valleys, forming a high plains scenery, which is actually a false impression of the river. These mountains are the watershed and the main source of Golmud River, Yangtze River, Za'gya Zangbo, Nujiang River, and Yalu Tsangpo River and also contain alpine lakes and alpine swamps.

Mountains, rivers, and tectonic movement have shaped the landscape of the Qinghai–Tibet Plateau, which in turn determine the railroad conditions. High plains approximately 50–200 km long are usual between the watershed areas, which are low and even; The railway mostly passes through the valleys, with only few sections passing through the watershed. The terrain units are as follows.

2.2.1 Qaidam Basin (K814+500–DK845+400)

The area from Golmud to Nanshankou forms the Qaidam Basin southern edge alluvial plain, which is flat and inclined northward with a longitudinal slope of approximately 15%. This basin, whose altitude is 2800–3000 m, has little vegetation, and is part of the Gobi desert.

2.2.2 Valley Terrace North of Kunlun Mountains (DK845+400–DK940+500)

Between Nanshankou and Xiaonanchuan, the line mainly runs along the Golmud River and the Kunlun River Valley.

The area from Nanshankou to Kunlun Bridge is part of the Golmud River strath terrace of northern Kunlun Mountains. The modern riverbed of Golmud River is a sharply cut U-shaped cross-section channel with precipitous sides; it is 10–8 m wide, the longitudinal slope is 15–20%, and scarps on both sides are 35–50 m high. Some sections of the riverbed have developed deep valleys that are less than 4 m wide but up to 35 m deep. Beyond the channel scarps, the terrain is open and flat and the vegetation sparse, forming the Gobi desert.

From Kunlun Bridge to Xiaonanchuan, the line runs along the valley terrace of Kunlun River, the upstream section of Golmud River. The modern riverbed is 20–200 m wide. The third terrace of Kunlun River is relatively complete and is 30–50 m above the riverbed. The first terrace is 3–10 m above than riverbed, and most of the second terrace is missing. The upper and middle reaches of Kunlun River exhibit cross-flow. The widest part of these flows is in Xiaonanchuan River area, which has a broad and shallow riverbed.

2.2.3 Xidatan Structural Valley (DK940+500–DK973+700)

The Xidatan valley is a flat terrain 30–50 km long (east to west) and 4–7 km wide (south to north). The line passes through the Xidatan basin from east to west at an altitude of 4120–4600 m. The northern boundary of the permafrost is located in DK957+640 at a high altitude of 4360 m.

2.2.4 Kunlun Medium-High Mountain Area (DK973+700–DK1005+500)

The Kunlun medium-high mountain area (4500–4800 m elevation) comprises Luanshi Ditch, which is on the northern slope of Kunlun Mountains; Kunlun Bealock; Kunlun Pass Basin; and Budongquan Valley. The terrain has large undulations, sparse vegetation, and dominant geomorphological features, such as ancient glaciers, modern glaciers, and frost weathering; alluvial and pluvial terraces are also present in some areas. Luanshigou Ditch is narrow and steep. Glaciofluvial deposition and lake basins are present in Kunlun Mountain Bealock and southern bealock area, and the terrain is relatively flat. Moreover, some harmful frozen-soil phenomena occur in this region.

2.2.5 Chumar River High Plains (DK1005+500–DK1072+500)

With an altitude of 4500–4700 m, the Chumar River high plains comprise the alluvial plains of Baladacai Qu, Qingshui River, and Chumar River. The topographical relief is low, with alterations of low hills and depressions; the vegetation is relatively rich. In addition to sandy lands and sand dunes, this area has thaw lakes and ponds. The valleys are characteristic of braiding and wandering river systems, and the stream trenching is indistinctive.

2.2.6 Hoh Xil Mountains (DK1072+500–DK1124+500)

The Hoh Xil Mountain area comprises the southern shore of Chumar River, Wudaoliang, Hoh Xil Mountains, Hongliang River, and Qushui River. The terrain is dissected by ravines and ridges and has wavelike undulations from southern Chumar River to Hoh Xil Mountains. Hoh Xil Mountains are spread out nearly east–west, with peaks at 4500–4700 m elevation; the ridges are gentle, with a

relative elevation of 100–300 m. Furthermore, fluid dunes are distributed in Hongliang Valley.

2.2.7 Beilu River Basin (DK1124+500–DK1145+500)

Located at a high altitude of 4500 m, the Beilu River Basin comprises Xiushuihe and Beilu River beach land and terrace and can be described as alluvial high plains. Topographical relief is low, with interphasing low hills and depressions. This region has gullies, the vegetation is sparse, and some areas have sandy lands and sand dunes.

2.2.8 Fenghuo Mountain Area (DK1145+500–DK1165+500)

With an altitude of 4500–4700 m, the Fenghuo Mountain area comprises Fenghuo Mountain Piedmont hill and its low mountain areas, with relative elevations of 200–300 m. The bedrock is exposed at the mountain summit; the ridge is gentle, with the upper regions of the hillside being precipitous and the lower regions flat. In addition, this region has intermontane valleys, with deep and precipitous slopes. The mountain area has a flat summit with gentle slopes, wide valleys, and short ditches.

2.2.9 Chiqu Valley (DK1165+500–DK1193+200)

The Chiqu Valley area has an altitude of 4580–4600 m and mainly comprises Chiqu River terraces, which has a flat terrain, developed ditches, and sparse vegetation.

2.2.10 Wuli Basin (DK1193+200–DK1202+500)

The Wuli Basin area mainly comprises alluvial and pluvial basins and has an elevation of 4580–4600 m; the area within the basin is flat and has sparse vegetation and a few ditches.

2.2.11 Wuli Mountain (DK1202+500–DK1217+700)

The Wuli Mountain region mainly comprises Wuli low mountains. It has an elevation of 4500–4700 m and has precipitous slopes and many deep-cut gullies. The bedrock is exposed, the summit flat, and vegetation sparse.

2.2.12 Tuotuo River Basin (DK1217+700–DK1245+000)

The Tuotuo River basin is broad in the east and narrow in the west, with alluvial fans and the Tuotuo River Valley and Terraces distributed in the marginal and central regions, respectively. This basin has sparse vegetation coverage, wide sand distribution, and low terrain undulation.

2.2.13 Kaixinling Mountain Area (DK1245+000–DK1252+800)

The peak of Kaixinling Mountain is flat and round, the slopes precipitous, and the gullies cut deeply. The intermountain basin is relatively flat, with wide vegetation coverage.

2.2.14 Tongtian River Basin (DK1252+800–DK1282+800)

The Tongtian River Basin mainly contains alluvial and diluvial plains, which comprise valleys and terraces, at 4600–4700 m elevation; the open and flat basin has a few sandy lands and sparse vegetation.

2.2.15 Buqu Valley (DK1282+800–DK1360+800)

Buqu Valley, elevation 4700 m, mainly comprises Buqu Valley, its floodplain, its first and second terraces, and an occasional third terrace. Encompassed by southern and northern mountains, this narrow valley runs south–north.

2.2.16 Wenquan Fault Basin (DK1360+800–DK1394+800)

Wenquan Basin is an N–S-trending extensional fault basin with a high altitude of 4700–4800 m, length of approximately 30 km (south–north), and width of 5–8 km. Its ambient areas contain greatly developed alluvial and diluvial fans. The Buqu riverbed is wide and shallow. This smooth-terrain area has numerous ditches and sparse vegetation coverage.

2.2.17 Tonglha Mountains and Intermontane Basin (DK1394+800–DK1485+200)

Tonglha Mountains, elevation 4700–5200 m, can be divided into three sections: the gorge area of the source of Buqu, the piedmont glaciofluvial deposit plain, and the mountainous and hilly regions.

1. Gorge area of the source of Buqu (DK1394+800–DK1419+300)—This area is 4800–5200 m high. The river channel in this area is curvy and narrow, with steep slopes, incomplete terraces, gullies, and sparse turfs. The topographical relief is slightly high, with exposed bedrock and thin Quaternary coverage.
2. Piedmont glaciofluvial deposit plain (DK1419+300–DK1458+700)—On this wide plain, surface runoff develops as a cross-flow, and no distinct gullies are present. Vegetation is sparse, and the ground glaciofluvial deposit layer is soft and difficult to walk on during the rainy season. Some thermokarst lakes are also present.
3. Mountainous and hilly regions (DK1458+700–DK1485+200)—This region has high topographical relief and sparse vegetation. Za'gya Zangbo River runs windingly in this region, but no river terraces are obvious. Moreover, this region has glacial deposits.

2.2.18 Touerjiu Mountain Area (DK1485+200–DK1513+770)

The landform of the Touerjiu Mountain Yueling area (elevation 4800–5100 m) is of the medium alpine landform, which is not very flat; it has numerous gullies and grooves and high vegetation coverage. Furthermore, permafrost swamping wetlands are present in the gully and slope area. Along the Galebu Meander, the landform becomes a V-shaped valley with a shallow riverbed and inconspicuous terraces.

2.2.19 High Plains Area in Northern Tibet (DK1513+770–DK1801+100)

The high plains area in northern Tibet, elevation 4600–4800 m, can be divided into two sections: the gorge area of the source of Duopuer Meander and the Anduo Senlis Valley.

1. Gorge area of the source of Duopuer Meander (DK1513+770–DK1801+100)—Gullies have developed in the area between Amdo and the source of Duopuer. Most of the bedrock on the shore is exposed. The riverbed is narrow, and mountains on both sides of the gorge are precipitous. Swamping wetlands are distributed on the gentle slopes.
2. Anduo Senlis Valley (DK1520+100–DK1801+100)—The major landforms along the Qinghai–Tibet Railway are piedmont alluvial plains, half-fixed sandy lands on the east coast of Beisang Qu, barchans on the east coast of Cuona Lake in Nagqu Valley, east coast alluvial plains and hills, and alluvial plains and hummocky moraine in Muge Qu. The general topography can be described as highland hills characterized by a gentle hillside, rare mountain peaks, inconspicuous gorges, and precipitous mountains with relative elevations of 300 m. The flat and open area between the mountains and hills contain alluvial, till, and lacustrine plains; drainage networks; wide and shallow riverbeds; and rivers with receding banks; large lakes; and strip wetlands, with high vegetation coverage of 60–90%.

2.2.20 Medium-High Mountain Area Between Samli and Yangbaling (DK1801+100–DK1904+500)

Located at a high altitude of 4200–4700 m, the medium-high mountain area between Samli and Yangbaling contains the Sang Qu medium-high mountain strath terrace, Jiuzina Mountain area, Damxung Basin, and Yangbaling piedmont alluvial plains.

1. Northern Jiuzina area (DK1801+100–DK1808+500)—The Qinghai–Tibet Railway line passes through Samli medium-high mountain strath terrace, which has a low and gentle surface relief, nearly 10‰ lateral ground slope, and sparse vegetation coverage.
2. Jiuzina Mountain area (DK1808+500–DK1810+000)—This area is affected by weathering, erosion, and tectonic movement and has the characteristics of a ridgelike landform, such as low hills, steep lateral slope, and sparse vegetation coverage.
3. Area between Jiuzina and Yangbaling (DK1810+000–DK1904+500)—The main geomorphology in this area are intermontane valleys and clinoplains, which are broad and flat. The valley is 10 km wide, on either sides of which are

high mountains with steep slopes and exposed bedrocks. The valley terrace is smooth, with lateral slopes of 2–6‰. Low terraces and floodplains can also be seen.

2.2.21 *Southern Nyainqentanglha Mountain Area from Yangbaling to Lhasa (DK1904+500–DK2006 +700)*

The southern Nyainqentanglha Mountain area, elevation 630–4600 m, contains Yambajan Basin, Doilung Qu Gorge area, and Lhasa River strath terrace.

1. Yambajan Basin (DK1904+500–DK1921+500)—This basin is 6–10 km wide (south–north) and tens of kilometers long (east–west). The Qinghai–Tibet Railway line passes through a broad and flat section of the basin, which also has floodplains and low terraces.
2. Doilung Qu Gorge area (DK1921+500–DK1993+500)—Also known as Yambajan Canyon, this gorge area has a relative height difference between the stream valley and banks of 500–1000 m and bank slopes of 35°–40°. The present riverbed is 20–50 m wide, with a longitudinal slope of 15–25‰; the valley is narrow and precipitous and sees rapid flow. The valley is 1–3 km wide, gradually becoming wider as it approaches Lhasa. The present riverbed is 100–300 m wide, with a longitudinal slope of 2–10‰. Terraces and ancient alluvial fans are present on each bank, but most of these are currently being utilized as farmlands.
3. Strath terrace in Lhasa River (DK1993+500–DK2006+700)—This terrace is 4–6 km wide (south–north), with the relative height difference of the banks being 500–800 m. The present riverbed is 500–800 m wide, with a longitudinal slope of 1–1.5‰. The riverbed is not very stable, and the mainstream flow varies widely.

2.3 Formation Lithology

The main strata along the Qinghai–Tibet Railway comprise the Quaternary system, Tertiary system, Cretaceous, Jurassic system, Triassic system, Permian system, Paleozoic group, Silurian system, Sinian system, lower Proterozoic, Caledonian granite, and magmatic rocks. The following sections describe the main strata along the line (i.e., from Golmud to Lhasa) from the newest to the oldest layer.

2.3.1 Quaternary System

2.3.1.1 Holocene Series

1. Silty clay ($Q_4^{al2, pl2, dl2}$)—Silty clay, mainly distributed in river terraces, piedmont alluvial plains, and the gentle surface layer, is 0.5 m thick on average and up to 10 m thick in the lacustrine plains between Amdo and Samli. This light yellow or tan clay is a flow plastic-to-hard-plastic grade II soft rock, with a bearing capacity (σ_0) of 80–150 kPa. On freezing, it becomes a grade IV soft rock with $\sigma_0 = 250$ –350 kPa.
2. Silt soil ($Q_4^{al3, pl3, dl3}$)—Silt soil is mainly distributed in river terraces, piedmont alluvial plains, and the gentle surface layer. The average thickness of the predominantly light yellow soil layer is 0.5–5 m. This prevalent grade II soil is in a slightly wet-to-saturated state, with $\sigma_0 = 80$ –150 kPa. On freezing, it becomes a grade IV soft rock with $\sigma_0 = 250$ –400 kPa.
3. Silt and fine sand ($Q_4^{al4, pl4, dl4}$)—occurring as lens-shaped, silt and fine sand are mainly distributed in the river floodplains and terraces and piedmont alluvial plains. On hillsides, these sands are primarily distributed on the surface, with a typical thickness of less than 5 m. This grade I loose soil is light yellow or steel-gray, loose-to-medium dense, and wet-to-saturate, with $\sigma_0 = 100$ –200 kPa. On freezing, it becomes a grade IV soft rock with $\sigma_0 = 250$ –450 kPa.
4. Silt and fine sand (Q_4^{eol4})—Silt and fine sand distributed are mainly distributed in the following areas: the gentle slope zone from Kunlun River to Naij Tal, some areas between Budongquan and Hoh Xil area as well as the local segment between Wuli and Kaixinling, the surface of piedmont alluvial plains from Tongtian River to Yanshiping, Cuona Lake area, and Lhasa River Valley terrace. In addition to the local dune chains and meniscus dunes, the vast majority of landform comprises half-fixed sandy lands and semifixed sand dunes. This prevalent grade II sand is loose, less than 5 m thick, light yellow or steel-gray, and slightly wet-to-wet.
5. Coarse sand ($Q_4^{al5, pl5, dl5}$)—Occurring as lens-shaped intercalates, coarse sand is mainly distributed in floodplains, terraces, and alluvial and diluvial plains. This stratum is less than 5 m thick and is light yellow or steel-gray, loose-to-medium dense, and slightly wet-to-saturated. It is a grade I loose soil, with σ_0 of medium sand being 150–300 kPa, and that of coarse and gravelly sand being 200–300 kPa. On freezing, it becomes a grade IV soft rock with $\sigma_0 = 300$ –600 kPa.
6. Thick pellet soil and brecciated soil ($Q_4^{al6, pl6, fgl6, dl6}$)—Thick pellet soil and brecciated soil are mainly distributed in river terraces, Xidatan and Chumar River high plains, alluvial plains, glaciofluvial deposit plains, and the surface layer of gentle slopes. The thickness of the strata with alluvial features can exceed 10 m, whereas that of the slope-made strata is less than 5 m. This prevalent grade II light yellow or dust-colored soil is loose-to-medium dense

and slightly wet-to-saturated, with $\sigma_0 = 300\text{--}400$ kPa. On freezing, it becomes grade IV soft rock with $\sigma_0 = 400\text{--}600$ kPa.

7. Cailloutis soil ($Q_4^{\text{al7, pl7, fgl7, dl7}}$)—Cailloutis soil is mainly distributed in riverbeds, river terraces, Xidatan Basin, glaciofluvial deposit plains, and Muge Qu and Sang Qu alluvial plains. This loose-to-medium dense wet-to-saturated soil stratum is >10 m thick. It is a grade III stiff soil with $\sigma_0 = 500\text{--}600$ kPa. On freezing, it becomes a grade IV soft rock with $\sigma_0 = 800$ kPa.
8. Gravelly soil ($Q_4^{\text{col7, dl7}}$)—Gravelly soil is mainly distributed in the toe area of Golmud River valley slopes, ambient areas in the rock heap foreland and collapse bodies in Naij Tal, and other local piedmont slope toes in alluvial plains. This grade III stiff soil is medium dense and slightly wet-to-saturated, with $\sigma_0 = 500$ kPa. On freezing, it becomes a grade IV soft rock with $\sigma_0 = 800$ kPa.
9. Granular soil and boulder clay ($Q_4^{\text{al8, pl8, col8, dl8}}$)—Granular soil and boulder clay are mainly distributed in piedmont alluvial terraces, moraine hills, and the toe of slopes. The deposition layer is >10 m thick, and this steel-gray grade IV soft rock is medium dense and slightly wet-to-saturated, with $\sigma_0 = 600$ kPa. On freezing, it remains a grade IV soft rock but with $\sigma_0 = 800$ kPa.
10. Sinter (Q_4^{ch})—Sinter mainly appears in hot springs, the summit area of Tonglha Mountains, and ambient area in Amdo; sinter has a granular structure and is mainly composed of travertine; it is white or off-white, light, and semihard.
11. Humic soil (Q_4^{l})—Humic soil is mainly distributed in the wetland surface layer between Amdo and Lhasa. Comprised of turf, rotten roots, and silty clay, this dust-colored or gray flow plastic-to-soft plastic, grade I loose soil layer is $0.5\text{--}2$ m thick. This soil makes for a poor foundation and thus must be avoided during line selection.

2.3.1.2 Upper Pleistocene

1. Silty clay ($Q_3^{\text{al2, pl2}}$)—Silty clay is distributed in the high terraces and the ancient piedmont alluvial fans on both sides of Dam Qu and Doilung Qu. This prevalent grade II hard-plastic clay layer is $0.5\text{--}5$ m thick, is brownish yellow or light gray, has homogeneous mass, and has more clay and less gravel, with $\sigma_0 = 150$ kPa.
2. Silt and fine sand ($Q_3^{\text{al4, pl4, fgl4}}$)—Silt and fine sand are mainly distributed in the lower sections of Golmud River terraces, moraine hills from Nanshankou to Naij Tal, and some sections on the northern slope of Kunlun Mountains. This grade I loose soil layer is light yellow and less than 5 m thick; it is medium dense and wet-to-saturated, with $\sigma_0 = 150\text{--}200$ kPa. On freezing, it becomes a grade IV soft rock with $\sigma_0 = 500$ kPa.
3. Thick pellet soil ($Q_3^{\text{al6, pl6, fgl6}}$)—Thick pellet soil is mainly distributed in the lower sections of Golmud River terraces, the moraine hill from Nanshankou to Naij Tal, and the surface of till plain in southwest Amdo. This prevalent grade II

soil layer is >10 m thick, light yellow or steel-gray, medium dense, slight wet-to-wet, and occasionally semibonded, with $\sigma_0 = 400\text{--}600$ kPa.

4. Gravelly soil and cailloutis soil ($Q_3^{\text{al}7, \text{pl}7, \text{fgl}7, \text{dl}7}$)—Gravelly soil and cailloutis soil is mainly distributed in piedmont alluvial terraces, moraine hills between Golmud and Wangkun, high terraces, and the ancient piedmont alluvial fans from Damxung to Lhasa; this grade III stiff soil layer is steel-gray, >10 m thick, medium dense, and occasionally semibonded, with $\sigma_0 = 800$ kPa.
5. Granular soil and boulder clay ($Q_3^{\text{col}8, \text{dl}8}$)—Granular soil and boulder clay is mainly distributed in piedmont alluvial terraces, moraine hills, and the toe of slopes in Golmud to Wangkun; this steel-gray grade IV soft rock layer is >10 m thick and loose-to-medium dense, with occasional shale or calcareous cementation and $\sigma_0 = 800$ kPa.

2.3.1.3 Middle Pleistocene

1. Thick pellet soil ($Q_2^{\text{fgl}6}$)—Thick pellet soil is mainly distributed on both sides of Luanshi Ditch. This prevalent grade II, steel-gray, medium dense layer is >10 m thick, with $\sigma_0 = 300$ kPa. On freezing, it becomes a grade IV soft rock with $\sigma_0 = 600$ kPa.
2. Cailloutis soil ($Q_2^{\text{fgl}7}$)—Cailloutis soil is mainly distributed on both sides of Luanshi Ditch. This prevalent grade III soil layer, steel-gray, medium dense sediment layer is >10 m thick, with $\sigma_0 = 500$ kPa. On freezing, it becomes a grade IV soft rock with $\sigma_0 = 800$ kPa.
3. Boulder clay ($Q_2^{\text{fgl}8}$)—Boulder clay is mainly distributed on both sides of Luanshi Ditch and on the surface of the moraine hill from Amdo to Samli. This grade IV, steel-gray, medium dense sediment layer is >10 m thick, with $\sigma_0 = 700$ kPa. On freezing, it becomes a grade IV soft rock with $\sigma_0 = 800$ kPa.

2.3.1.4 Lower Pleistocene

Silty clay ($Q_1^{\text{l}2}$)—Silty clay is mainly distributed in Kunlun Pass Basin and Chumar River high plains. With a thickness of >5 m, this prevalent grade II clay is dust-colored or charcoal gray and has homogeneous mass, with $\sigma_0 = 100$ kPa. On freezing, it becomes a grade IV soft rock with $\sigma_0 = 250\text{--}350$ kPa.

2.3.2 Tertiary System

2.3.2.1 Neogene

Sandstone, mudstone, marl ($N^{\text{Ss+Ms+Am}}$)—Neogene, which is a light red or multi-colored continental sediment composed of sandstone, mudstone, and marl as well as

gypsum clastic rocks, are mainly distributed in Chumar River high plains, Togton River Basin, Tongtian River Basin, and Yanshiping and Buqu high terraces. The bottom section of this sediment is a thin layer of light-red quartz sandstone and sandstone, the middle section is composed of alternating layers of tangerine and gray-green sandstone and mudstone, and the top sections are an interbed of light-red sandstone with dust-colored or gray siltstone, atop which lies an interbed of gray marl and gray-yellow mudstone, respectively. The rocks in this sandy sedimentary soil are in a transition state between being fully weathered and strongly weathered. Neogene is a grade III stiff soil with $\sigma_0 = 150\text{--}200$ kPa, which on freezing becomes a grade IV soft stone with $\sigma_0 = 250\text{--}350$ kPa.

2.3.2.2 Lower Tertiary

Mudstone and sandstone (E^{Ms+Ss})—Mudstone and sandstone rocks are mainly distributed in Fenghuo Mountain area, where they appear as extra-thick alternating beds of heliotrope, dark red sandstone, and mudstone that been undergone different degrees of weathering. They are grade IV soft rocks surrounded by grade IV rocks, with $\sigma_0 = 250\text{--}350$ kPa.

2.3.3 Cretaceous

1. Sandstone (K^{Ss})—Sandstone is scattered in the area between Touerjiu and Amdo, the ambient area of Liangdaohe Army Service Station, the southern part of Jiuzina pass, and the area between Yambajan and Sai Qu. The sandstone here is purplish-red and is interbedded with shale and conglomerate. The regolith is 3–5 m thick, and these weathered rocks are grade IV soft rocks with $\sigma_0 = 400\text{--}600$ kPa, whereas the whole bedrock is grade V secondary hard rock with $\sigma_0 = 800$ kPa.
2. Conglomerate (K^{cg})—Conglomerate is distributed along the left bank of Nagqu and has the following characteristics: bedded structure, fragmental texture, calcium and mud cementation, numerous joints, crushed rocks, and strongly weathered-to-weakly weathered. The regolith is 2–4 m thick; this rock is grade IV soft rock with $\sigma_0 = 500$ kPa. The bedrock is grade V secondary hard rock with $\sigma_0 = 800$ kPa.
3. Limestone (K^{ls})—Off-white and hard limestone is scattered in the area between Touerjiu and Amdo, with regolith of thickness 1–3 m; this grade IV soft rock has $\sigma_0 = 800$ kPa. The whole bedrock is grade V secondary hard rock with $\sigma_0 = 1000$ kPa.

2.3.4 *Jurassic System*

1. Mudstone interbedded with shale (J^{Ms+Sh})—Mudstone interbedded with shale is mainly distributed in Yanshiping to Amdo. These stratified rocks have alternating light gray and brownish-red layers and exhibit calcium and mud cementation. Varying from fully weathered-to-strongly weathered, the regolith is 3–5 m thick and is grade IV soft rock with $\sigma_0 = 400\text{--}600$ kPa. The whole bedrock is grade V secondary hard rock with $\sigma_0 = 600\text{--}800$ kPa.
2. Sandstone interbedded with shale (J^{Ss+Sh})—Sandstone interbedded with shale is distributed between Yanshiping and Amdo, the upper low-alpine sections between Amdo and Samli, between Samli and north Damxung, and in the northern Doilungdêqên. These purplish-red and gray-green sediments have thin layer construction and an arenopelitic structure. The regolith is 3–5 m thick grade IV soft rock with $\sigma_0 = 400\text{--}600$ kPa. The whole bedrock is grade V secondary hard rock with $\sigma_0 = 800$ kPa.
3. Limestone (J^{ls})—Off-white and hard limestone is mainly spread between Yanshiping and Amdo and in the ambient area of Doilungdêqên. The regolith is 1–3 m thick and is grade IV soft rock with $\sigma_0 = 800$ kPa. The whole bedrock is grade V secondary hard rock with $\sigma_0 = 1000$ kPa.
4. Gypsum bed (J^{gy})—Soft, fragile, and white gypsum bed, of type grade IV soft rock, is mainly spread in the Wenquan Valley area.

2.3.5 *Triassic System*

Comprised of schist, slate, sandstone, phyllite, and limestone, the Triassic system is mainly distributed in Budongquan, Wudaoliang, and Wuli Mountain area. Alternating beds of limestone and chert have developed in Tongtian River Small Bealock.

1. Schist (T^{Sc})—Schist in this system is dark red, gray-red, and brown, with fractures, joints, and crushed rock stratum. Exhibiting weak weathering, this schist is grade IV soft rock and grade V secondary hard rock with grade IV surrounding rock and $\sigma_0 = 400\text{--}600$ kPa.
2. Slate (T^{Sl})—Slate in this system is dark red, gray-red, and brown, with fractures, joints, and crushed rock stratum. Exhibiting weak weathering, this slate is grade IV soft rock and grade V secondary hard rock with grade III and IV surrounding rock and $\sigma_0 = 600$ kPa.
3. Sandstone (T^{Ss})—Sandstone in this system is dark red and gray-red with fractures, joints, and crushed rock stratum. Exhibiting weak weathering, this sandstone is grade IV soft rock and grade V secondary hard rock with grade III and IV surrounding rock and $\sigma_0 = 800$ kPa.
4. Phyllite (T^{Ph})—Phyllite in this system is dark red, with fractures, joints, and crushed rock stratum. Exhibiting weak weathering, this phyllite is grade IV soft rock with grade III and IV surrounding rock and $\sigma_0 = 400\text{--}600$ kPa.

5. Limestone (T^{lh})—In this system, limestone is interbedded with chert layer. These hard and off-white limestone sediments have 1–3-m-thick regolith and are grade IV soft rock with $\sigma_0 = 800$ kPa. The whole bedrock is grade V secondary hard rock with $\sigma_0 = 1000$ kPa.

2.3.6 Permian System

The Permian system outcrop area is mainly located in Luanshi Ditch, Wuli Mountain, and Kaixinling. The main lithology of Permian system is slate, schist, sandstone, shale, limestone, and phyllite.

1. Slate (P^{Sl})—Slate, presenting as gray-green or yellow-green, has joints, fractures, and weak regolith. This slate is grade IV soft rock and grade V secondary hard rock with grade III and IV surrounding rock and $\sigma_0 = 600$ kPa.
2. Schist (P^{Sc})—Schist, presenting as gray-green or yellow-green, has joints, fractures, and weak regolith. This schist is grade IV soft rock and grade V secondary hard rock with grade III and IV surrounding rock and $\sigma_0 = 400$ –600 kPa.
3. Sandstone (P^{Ss})—Sandstone, presenting as gray-green or steel-gray, exhibits joints and fractures and weak weathering. This sandstone is grade IV soft stone and grade V secondary hard rock with grade III and IV surrounding rock and $\sigma_0 = 800$ kPa.
4. Shale (P^{sh})—Shale, presenting as gray-green or gray, has fractures and joints and weak weathering. This sandstone is grade IV soft rock with grade IV surrounding rock and $\sigma_0 = 400$ kPa.
5. Limestone (P^{ls})—The gray and off-white limestone in this system is grade V secondary hard rock with and joints and fractures and $\sigma_0 = 1000$ kPa.
6. Phyllite (P^{ph})—Phyllite, presenting as gray-green or yellow-green, has fractures, joints, and crushed rock stratum. This weakly weathered phyllite is grade IV soft rock with grade IV surrounding rock and $\sigma_0 = 400$ –600 kPa.

2.3.7 Paleozoic Group

With the main lithology of low metamorphic schist, sandstone, and limestone, the Paleozoic group mainly occurs as outcrops in the southern Dagangou Bedrock Mountain area and low mountain area. Granitic gneiss outcrops can be seen in Beisang Meander, the northern shore of Cuona Lake, and Yambajan.

1. Schist (P_z^{Sc})—This group contains chlorite schist, sericite-quartz schist, tremolite, and actinolite schist, which are gray or gray-green with high schistosity and numerous joints. Squeezing movement has distorted the strata, and part of the

rock surface is severely weathered. These schist are grade IV soft rocks with grade III and IV surrounding rock and $\sigma_0 = 600\text{--}800$ kPa.

2. Sandstone (P_z^{ss})—Sandstone, presenting as gray-green or gray, has joints and fractures and weak-to-strong weathering. These sandstones are grade IV soft rocks and grade V secondary hard rocks with grade III and IV surrounding rock with $\sigma_0 = 800$ kPa.
3. Limestone (P_z^{ls})—Limestone, coral, and other fossils can be found in gray or gray-green hard limestone. This limestone has joints and fractures and is mainly distributed near Naij Tal. It is a grade V secondary hard rock with grade V surrounding rock and $\sigma_0 = 1000$ kPa.
4. Granitic gneiss (Gn)—This system has off-white or gray-black granite sediments that exhibit a gneissic structure. The regolith is 1–5 m thick and is grade IV soft rock with $\sigma_0 = 500$ kPa. The whole bedrock is fifth-grade secondary hard rock with $\sigma_0 = 1000$ kPa.

2.3.8 Magmatic Rocks

1. Granite (γ_4, γ_5)—Granite γ_4, γ_5 in north Dagangou is formed in Variscan and that in the south in Yanshanian period. It is off-white or pale red with a medium-grained texture. These strong-to-weak weathered granites with joints and fractures are grade V secondary hard rock with $\sigma_0 = 1000\text{--}1200$ kPa.
2. Granite (γ_6)—Granite γ_6 is mainly distributing in Yambajan tunnels 1 and 2, in Liuwu tunnel, and from Gurong to Lhasa. This off-white or pale red granite has a massive and medium-coarse-grained structure with many joints. This 3–8-m-thick strongly weathered layer is grade IV soft rock with $\sigma_0 = 500$ kPa. The weakly weathered layer and the whole bedrock are grade V secondary hard rocks with $\sigma_0 = 1000$ kPa.
3. Gabbro (ν) and andesite (α)—Gabbro and andesite are mainly distributed in Kaixinling, Duopuer Meander, and Yangbaling. They are off-white or gray-black with an equigranular texture and a massive structure. This 2–4-m-thick strongly weathered layer is grade IV soft rock with $\sigma_0 = 500$ kPa. The weakly weathered layer and the whole bedrock are grade V secondary hard rocks with $\sigma_0 = 1000$ kPa.

2.4 Geological Structure

The Qinghai–Tibet Railway passes through the head of the Qinghai–Tibet Plateau eta-type tectonic system. Most of this area features intense uplift geosynclines, and linear fractures appear in bundles. The strata include many folds and faults from the Sinian Suberathem, and the new tectonics (mainly fractures) show obvious

inheritance from and reconstruction of the old fractures with strike faults. In each generation, different tectonic movements generate different fracture systems.

The main folds along the Qinghai–Tibet Railway are the Naij Tal Anticlinorium, Hoh Xil Synclinorium, Fenghuo Mountain Syncline, Kaixinling Anticline, Tonglha Mountain Synclinorium, Amdo Arc Fault–Fold Belt, and Nagqu Compound Fold–Fault Belt.

The main faults along the line are the Golmud Concealed Fracture, Xidatan Concealed Compressive Fracture, Kunlun Mountains Bealock Compressive Shear Faults, the Northern Fenghuo Mountain Compressive Fracture, Wuli Fracture Zone, Yanshiping Regional Compressive Shear Faults, Tonghla Mountain Fault Zone, the Eastern Shore Fault at Cuona Lake, and the Nagqu–Damxung–Yambajan Fault Zone.

2.4.1 Folds

2.4.1.1 Naij Tal Anticlinorium

Located in the northern slope of Kunlun Mountains, Naij Tal Anticlinorium is a linear angular overturned and composite anticline comprised of Paleozoic metamorphic rocks. The nearly EW-trending axis of the anticline in the area from Naij Tal to Kunlun Bridge was formed in the Caledonian.

2.4.1.2 Hoh Xil Synclinorium

Belonging to Hoh Xil–Qumarlêb Synclinorium, the Hoh Xil Synclinorium has a NWW–SEE axis. The tightly distributed folds consist of the Late Triassic Bayanhar Group formed in the Indosinian.

2.4.1.3 Fenghuo Mountain Syncline

Fenghuo Mountain Syncline is comprised of lower Tertiary rocks formed in the Himalayan period. The axial direction of this gentle branchy syncline is nearly NW–SE, and the dip angle of axial part strata is less than 20°. The development of the north wing is incomplete because of fracture cutting, whereas the south wing has developed two secondary synclines. The axial direction of the first syncline is uncoordinated with the main syncline.

2.4.1.4 Kaixinling Anticline

With a nearly NS–SE axial direction, Kaixinling Anticline comprises the Permian system, with sandstone composing the axial section and limestone composing the two wings, which are almost identical. This anticline was formed in the Late Hercynian and was reformed by the late tectonic activity.

2.4.1.5 Tonglha Mountain Synclinorium

Tonglha Mountain Synclinorium is around 200 km long in the south–north direction. With a NW–SE axial direction, this synclinorium is composed of the Yanshiping group and was formed in the Early Yanshanian period. Five secondary synclines—Yanshiping, 102 Road, 104 Road to 106 Road, 111 Road, and 114 Road to 115 Road—and four secondary anticlines—Wenquan Military Depot, 103 Road, Tonglha Main Ridge, and Touerjiu Mountain—constitute the Tonglha Mountain Synclinorium.

2.4.1.6 Amdo Arc Fault–Fold Belt

Amdo Arc Fault–Fold Belt is composed of north Amdo Mountain and an arc structural valley, which has complex structural features: The arc roof is a convex northward arc structural belt, with the outer arc uplifted forming a high mountain; the dropped inner arc forms the valley.

2.4.1.7 Nagqu Compound Fold–Fault Belt

With similar anticlines and synclines and two symmetrical wings, Nagqu Compound Fold–Fault belt is distributed south of the Qinghai–Tibet Highway 126 Road, a nearly EW-trending undulate fold. The formation of these folds was accompanied by the formation of a few small nearly EW–NEE-trending fractures.

2.4.2 Faults

2.4.2.1 Golmud Concealed Fracture (F1)

The 400-km-long Golmud Concealed Fracture, a segment of Urt Moron–Nomuhong Concealed Fracture, lies to the south of Golmud. The Quaternary system in the southern and northern walls of the fault is 621 and >1000 m thick, respectively. Because of this fault, the Qinghai–Tibet Railway line from Golmud to Nanshankou is built as an embankment.

2.4.2.2 Xidatan Concealed Compressive Fracture (F2)

Located in the Xidatan Structural Valley, Xidatan Concealed Compressive Fracture is a part of Kunlun Lake–Xiugou Deep Fault, and it controls the southern boundary of the Paleozoic group. Magmatic intrusions are present along the fault, and the fracture surface is buried 300 m beneath the Quaternary. In this region, the Qinghai–Tibet Railway line has mainly used embankments.

2.4.2.3 Kunlun Mountains Bealock Compressive Shear Faults (F3)

1. D6-F1 and D6-F2 Compressive Fracture—This fracture is located in the valley area near the entrance of the Kunlun Mountains tunnel and intersects the Qinghai–Tibet Railway at DK976+058 and DK976+158. The D6-F1 fault strikes N72°W and dips southward; Quaternary deposits cover its surface, and the fault fracture zone is approximately 45 m wide. The D6-F2 fault strikes almost EW and dips 50°–70° northward; Quaternary deposits cover its surface. The fault fracture zone is about 50 m wide and consists of broken phyllite and slate, which was also found in the D6Z-247 drilling core. The railway line uses culverts to pass through this fault area, and the fractures slightly affect railway engineering in this area.
2. D6-F3 Compressive Fracture—This fracture, located north of Kunlun Mountains Bealock, intersects the line around DK979+520 at 45°. The fault strikes N75°W and dips northward at 70°–80°; Quaternary deposits cover its surface, and fault fracture zone is 20–27 m wide. Stratum lithology in the northern wall of the fault consists of Triassic slate with schist, and denudation in the southern wall of the fault has exposed Lower Pleistocene lacustrine silty clay and silt. The fault was activated again by the Kunlun Mountain Pass Earthquake on November 14, 2001. The Qinghai–Tibet Railway used embankments to pass through this fault area, and the fractures slightly affect railway engineering in this area.
3. D6-F4 Compressive Fracture—This fracture is distributed north of Kunlun Mountains Bealock, in the southern Kunlun Ditch. This normal fault intersects with the Qinghai–Tibet Railway line at 45° near DK981+850. The fault strikes N62°W and dips northward at 50°. The fault fracture zone is approximately 30 m wide and consists of broken phyllite and slate. Stratum lithology in the northern wall of the fault is Triassic slate with schist, and denudation in the southern wall has exposed Lower Pleistocene lacustrine silty clay and silt. The Qinghai–Tibet Railway line uses bridges to pass through this fault area.

2.4.2.4 Northern Fenghuo Mountain Compressive Fracture (F4)

Distributed in the north piedmont of Fenghuo Mountain and intersecting with the Qinghai–Tibet Railway in DK1147+420, the Northern Fenghuo Mountain

Compressive Fracture strikes almost NE and dips southward at 70°–85°; the fault zone is nearly 600 m wide. This fracture, produced in the Tertiary strata, is a part of Xijir Ulan Lake–Dam Qu Fracture, and the fault controls the upper Triassic Jieza group and the northern boundary of the Jurassic strata. The Qinghai–Tibet Railway line uses low embankments to pass through this fault zone, and the fracture has little influence on local railway engineering.

2.4.2.5 Wuli Fracture Zone (F5)

Wuli fracture zone is distributed in the piedmont area of Wuli Mountain and intersects the Qinghai–Tibet Railway line in DK1202+620 and DK1202+716. The fault strikes almost N78°W, and its surface is covered by Quaternary deposits. The fault fracture zone is approximately 96 m wide. Unfavorable geological phenomena, such as island taliks, hot springs, and frost mounds, are present along the fracture belt. The railway line uses bridges to pass through this fault area, and the fractures slightly affect railway engineering in this area.

2.4.2.6 Yanshiping Regional Compressive Shear Fault (F6)

Located in Yanshiping region, the Yanshiping Regional Compressive Shear Fault zone comprises a series of parallel faults and is hundreds of kilometers long. It controls the distribution of the Jurassic strata. In this area, the Qinghai–Tibet Railway line passes through seven buried faults, all of which are nearly orthogonal to the line (see Table 2.3). The D3-F1 fault, located in the Chaqingqu Bridge area, strikes almost N30°W and dips southward at 72°. The fracture affects bridge engineering here to some extent: in particular, the D3-F5 fault is located in the area with the middle section of the bridge, which contains gypsum; therefore, engineering treatment of the foundation is essential.

Table 2.3 Relationship between the Yanshiping Fault Zone and the Qinghai–Tibet Railway line

Fault	Railway boundary marker	Fault properties	Fault–railway intersection angle
D3-F1	DK1336+730	Reverse fault	70°, dips to N
D3-F2	DK1337+920	Reverse fault	70°, dips to N
D3-F3	DK1340+490	Reverse fault	50°, dips to N
D3-F4	DK1342+290	Parallel displacement fault	Orthogonal
D3-F5	DK1343+920	Reverse fault	Orthogonal, dips to S
D3-F6	DK1348+050	Reverse fault	Orthogonal, dips to N
D3-F7	DK1350+230	Reverse fault	Orthogonal, dips to S

2.4.2.7 Tonghla Mountain Fault Zone (F7)

The main strike of the Tonghla Mountain Compressive Fracture lies NWW and NE. Presenting as reverse faults and normal faults, the fault zone mainly occurs in the Mesozoic (Jurassic) strata, generally at an angle of 40° – 60° . The main faults are described herein

1. D12-F1—A reverse fault, D12-F1 fault is distributed from DK1358+900 to DK1359+020; the fault fracture zone is 120 m wide, occurring at $N69^{\circ}W/79^{\circ}S$ in the Jurassic strata. A gray–white gypsum layer constitutes the hanging wall of the fault, and a purplish-red conglomerate constitutes the footwall. A 10–20-m-thick Quaternary accumulation layer is present near the Qinghai–Tibet Railway; 200 m to the left of this line, the fault is exposed in the mountain slope, and the lithology is clear. No major projects have been implemented in the fault area. The railway line uses fills to pass through the fault zone, which slightly affects the railway engineering in this area.
2. D12-F12—Distributed around DK1360+000, the D12-F12 fault is a buried fault that strikes $N42^{\circ}E$ at a steep dip angle. Occurring in the Jurassic strata, the hanging wall of the fault consists of limestone and conglomerate, and the footwall consists of a gray–white gypsum layer. A 5–20-m-thick Quaternary accumulation layer is present near the Qinghai–Tibet Railway line. No major projects have been implemented in the fault area, which barely influences local railway engineering.
3. D12-F3—A buried normal fault, the D12-F3 fault ($N20^{\circ}E/60^{\circ}S$) lies to the right of DK1394+000. Occurring in the Jurassic strata, the lithology of this fault is mainly comprised of limestone, sandstone, and shale in this area. This fault is far from the Qinghai–Tibet Railway line, which uses subgrades to pass through the fault area; the fault exerts no effect on local railway engineering.
4. D12-F4—Distributed near DK1394+415–DK1394+430, the D12-F4 fault ($N35^{\circ}E/87^{\circ}S$) is a nearly 15 m wide buried fault. The fault fracture zone here contains fault breccia.
5. D12-F5—Occurring in the Jurassic strata, the D12-F5 fault is a buried reverse fault distributed near DK1396+300–DK1396+400. It strikes $N38^{\circ}E$ at a steep dip angle. The Buqu River Bridge is built in this fault region, which exerts a slight effect on local railway engineering.
6. D12-F5—Distributed in DK1398+400, the D12-F4 fault is a buried reverse fault present in the strata of Jurassic sandstone, shale, and limestone formations. It occurs at $N39^{\circ}E$ and has steep dip angle. Quaternary deposits are present near the Qinghai–Tibet Railway line in this area. No major projects have been implemented in the fault area, which barely influences local railway engineering.

2.4.2.8 Cuona Lake Eastern Coast Fault (F8)

To the east of Cuona Lake Eastern Coast Fault, which trends NEE, is a mountain ridge composed of Yanshanian Granite and Paleozoic metamorphic rock, and to the west is Cuona Lake. The fault fracture zone is 30–40 m wide. The fault extends to the north and intersects the North Sangkarigang Fault on the east coast of Sangqu. Along DK1553+000–DK1557+900, the Qinghai–Tibet Railway line passes 100–200 m away from the fault on average, with the closest approach at DK1579+100–DK1580+000 (25–50 m) and DK1580+000–DK1581+000 (<20 m).

2.4.2.9 Nagqu–Damxung–Yambajan Fault Zone (F9)

1. Nyainqentanglha Mountain Eastern Marginal Fault (D9-F1)—This fault (SN45°–60°E) is a Holocene active fault that strikes almost SN from Sangshung to Jiuzina and NE–NEE from Jiuzina to Gariqiao. The Qinghai–Tibet Railway passes close to the fault between Sangshung Station and Jiuzina Flyover. The fault exerts some effect on local railway engineering. Chun Lang Bridge (DK1797+449) and Jiuzina No. 1 Bridge (DK1802+916) as well as subgrade engineering are present in this section.
2. Damxung Basin Northern Marginal Fault (D9-F2)—A part of the eastern Nyainqentanglha Mountain Marginal fault, this fault strikes nearly EW and dips southward. Left-lateral strike slip has been occurring since the Holocene, and the normal dip-slip component is evident. In DK1801+000, the Qinghai–Tibet Railway uses a roadbed to pass through the fault zone.
3. Langguo–Sangqu Fault (D9-F3)—Starting from the toe of Baguran Gully, this fault cuts through the toe of Ribalang Gully in the east before entering Sangqu Ditch. In west Baguran, this normal fault (N70°E/70°N) is buried in the piedmont alluvial plain. The Qinghai–Tibet Railway line passes through a belt influenced by the faults. Apart from the sections with the Ribalang Bridge (DK804+970) and Baguran Bridge (DK1813+116), the line uses roadbeds to pass through this area.
4. Eastern Boundary Fault of Damxung–Yambajan Graben—This 20 m wide fault (N65°E/70°N) is spread along the Qinghai–Tibet Highway, and most of the fault along the Qinghai–Tibet Railway line is buried. The railway line passes through the influence belt of this normal fault in the DK1831–DK1846 section, where Benla Bridge (DK1840+374) and Jiagen Bridge (DK1841+960) are built. The line uses roadbeds to pass through the rest of the fault zone.

2.5 Hydrogeology

2.5.1 Regional Hydrogeological Conditions

The hydrogeological conditions along the Qinghai–Tibet Railway is influenced by the local climatic characteristics, topography, lithology, geological structure, ancient and recent tectonic activities, and other natural factors. The permafrost zone along the line (Xidatan to Amdo) can be classified into various hydrogeological units with differing hydrogeological conditions

1. Permafrost of a certain thickness can form a relatively complete and uniform aquifuge, and different types of groundwater, such as suprapermafrost water, infrapermafrost water, and meltwater, differ in their distribution characteristics and enrichment regularity.
2. The groundwater in this area is mainly recharged by atmospheric precipitation, snowmelt water, and glacier-melt water. The surface water accumulates and develops into streams, and in the runoff process, this surface water replenishes the suprapermafrost water and groundwater in the nonpermafrost regions. The frozen layer in the permafrost region prevents the infrapermafrost water from being directly recharged by the surface water. In addition, infrapermafrost water is present in low quantities because it is replenished only by the suprapermafrost water or surface water from rivers and lakes or the bottom of melting glaciers. Moreover, only 10% of the atmospheric precipitation infiltrates the ground to replenish the groundwater, with the rest either evaporating or being discharged as surface runoff.
3. Suprapermafrost water is excreted in the thaw area, and the runoff is slow. The outcrop of natural infrapermafrost water forms ice cones and frost mounds in the cold season.
4. The region along the Qinghai–Tibet Railway line can be categorized as the four large groundwater catchment areas of Kunlun Mountains, Tonglha Mountains, and Nyainqentanglha Mountains, the hydrogeological conditions of which differ widely because of the differences in the formation lithology, structural features, and topography.
 - a. The region to the north of Kunlun Mountains is the groundwater area of Golmud Valley. Its hydrogeological environment is controlled by the latitudinal tectonic system. The bedrock here has fractures, and the valley is filled with loose gravel. The groundwater is of high quality, with a low mineralization degree and fast runoff.
 - b. The region from Kunlun Mountains to Tonglha Mountains is the high plains groundwater basin area of the source areas of the Yangtze River, where a range of alternating low mountains and faulted basins constitute an undulating plain. This region contains Permian coal bearing strata and Mesozoic salts. The groundwater is of poor quality, with high mineralization degree, poor supply, and slow runoff.

- c. The region to the south of Tonglha Mountains is the Za'gya Zangbo and Jiebu Qu groundwater area. Presenting as a series of stepped mountains, the hydrogeological environment here is controlled by an eta-type tectonic system. Clastic rocks and carbonate rocks of Middle Jurassic constitutes the main water-bearing strata. Groundwater is of high quality, with fast runoff.
 - d. Between Amdo and Samli, Quaternary pore phreatic water is mainly distributed in the valleys, plains, and interdune depressions. With a shallow depth of burial, the pore phreatic water is abundant and of high quality and is additionally supplied by surface water and atmospheric precipitation.
 - e. Between Samli and Lhasa, phreatic water is mainly distributed in the valley plain terrace and piedmont alluvial and diluvial plains; in bedrock fissures, water is distributed in the constituent sandstone and granite. Both the quantity and quality of this water is high.
5. Strong tectonic activities have formed structural valleys, mountains, and basins. These structural systems strongly influence the hydrogeological conditions in this area.
 - a. The bedrock mountain area with folds and fractures has effective water storage structures, and the water quality is high.
 - b. In the Early Cenozoic fault basin, the outwash sand gravel covering the layer is thin, and the groundwater is mainly hosted in the early Cenozoic lacustrine salt formation. The water quality is poor.
 - c. In the structural valley, the groundwater is mainly hosted in the very thick outwash gravel deposits that formed in the Late Cenozoic, and the water is abundant and of high quality.

2.5.2 Groundwater Type

2.5.2.1 Groundwater in Nonpermafrost Regions

Table 2.4 summarizes the types and distribution of groundwater in nonpermafrost regions.

2.5.2.2 Groundwater in Permafrost Regions

The permafrost layer in permafrost regions increases the complexity of the distribution and burial of groundwater. The groundwater in such regions can be classified into three types: suprapermafrost water, infrapermafrost water, and meltwater.

1. Suprapermafrost water

Widely distributed in the permafrost regions of the Qinghai–Tibet Plateau, suprapermafrost water has an unstable water level and a changing phase state, with

Table 2.4 Characteristics of groundwater in nonpermafrost regions

Groundwater type		Distribution and burial	Features
Phreatic water	Pore water	Distributed in the valleys of Amdo, Xidatan, and Golmud River; alluvial and flood fans of Golmud River; and the pores of diluvial and ice-water sand gravel	High quantity and quality; most are related to river water
	Fissure water	Distributed in the weathering and structural cracks of igneous rock, metamorphic rock, sandstone, and shale in Kunlun Mountains and Tonglha Mountain area	Relatively high quality water, with uneven abundance
Piestic water	Karst water	Distributed in the fractures of marble and magmatic rocks in Kunlun River Valley	High quality and quantity
	Pore water	Interlayer water distributed in the toe of alluvial and flood fans in Golmud River	High quality and average quantity
	Fissure water	Distributed in the hanging wall of compressive fault zones in rocky mountains and the intersection of fracture zones with different mechanical properties	High quality and quantity

the burial conditions and water volume varying with the season. The thickness of the aquifers is controlled by the upper limit of the permafrost.

In this area, the upper limit depth of the permafrost is generally 1–3 m, and the aquifers have low thickness (~ 1 m). The distribution of the supraperafrost water is affected by the runoff and vertical evaporation and is thus controlled by the topography; unified aquifers cannot form in higher grounds. In early April, the ground begins to thaw. The consequent melting of the ice body in the soil results in the gradual formation of a water-bearing layer in the active layer. By late September–early October, the thaw depth reaches the limit value, and the aquifer attains its peak thickness. By this time, the ground layer begins to freeze, and the frozen depth gradually increases until January; the soil layer remains completely frozen and connected to the permafrost at the end. Over the freezing period, the active zone of the groundwater becomes increasingly smaller, and the burial conditions change over time.

Supraperafrost water can change from phreatic water in warm season to confined water in the cold season. When the hydrodynamic pressure becomes adequate to break through the upper soil layer, the confined water may run out of the ground at fragile sections and freeze into ice cones; alternatively, the water may move toward a weak underground soil layer, transforming the raised upper soil layer into frost mounds.

Supraperafrost water is a type of phreatic water that is stored in a thin and unstable aquifer. Its burial and distribution is mainly determined by the distribution of the seasonal thawing layer and the baseplate shape of the permafrost meltwater.

2. Infrapermafrost water

A major form of groundwater in permafrost regions, infrapermafrost water has a stable phase state and is in a liquid state in all four seasons.

In addition to the edge of the Xidatan permafrost region, infrapermafrost water in this area is confined except in some places, where it may flow on to the surface. As the bearing roof, the thickness of the permafrost layer is directly influenced by the runoff conditions and the regularity of infrapermafrost water formation. This water has poor supply and runoff condition, mutable water quality, and highly nonuniform quantity.

The distribution of the infrapermafrost water is restricted by the permafrost layers. Depending on the characteristics of the water medium, the frozen layer can be classified as pore water, fissure water, pore–fissure water, and karst water (Table 2.5).

Table 2.5 Classification of infrapermafrost water

Groundwater type		Distribution and burial	Features
Pore water		(1) Distributed in glaciofluvial deposits and sandstone pores of the structural valleys of Xidatan, Wenquan, and Za’gya Zangbo, among others (2) Distributed in the half-diagenesis packsands and siltstone pores of fault basins of the Chumar River, Tuotuo River, and Tongtian River, among others	Water distributed in the ice-water sand gravel layer is abundant and of high quality whereas that distributed in the half-diagenesis layer is not
Pore–fissure water		Distributed in the mudstone and glutenite pores of fault basins in Hoh Xil Mountains, Fenghuo Mountain Piedmont, and Tongtian River, and Beilu River	Low quantity and quality, except in some fracture zones in the piedmont
Fissure water		Distributed in the structure cracks of igneous rocks, metamorphic rocks, sandstones, and shale in Kunlun Mountains and Tonglha Mountain Piedmont	Low quantity, except in the fault zone; quality varies widely
Karst water	Pore karst water	Distributed in the marl karst pores in the basins of Chumar River and Tuotuo River	Low quantity and quality
	Fissure karst water	Distributed in the karst fissures and pores of very thick carbonatite in Tonglha Mountain Piedmont	Relatively high quantity and quality

Table 2.6 Meltwater classification

Groundwater type	Talik type	Distribution and burial	Features
Piece melting zone water	Snow-covered talik	At the bottom of modern glaciers	High in quantity and quality; supplied by meltwater
	Lake talik	Around large lakes and at the bottoms of other lakes	High in quantity but of low quality; mostly from groundwater collection area
Zonal melting zone water	River talik	At bottom river beds and narrow strips of Tuotuo River, Tongtian River, and Buqu, among others	Structural fissure water in rocky mountains; pore phreatic water in basins and valleys; water quantity and quality is relatively high
Dotted melting zone water	Shallow circulating talik	At the intersection of shallow fractures and karst development zones	Mostly confined water of high quantity and quality and low temperature
	Deep circulating talik	At the intersection of deep fractures	Mostly confined water of high quantity and temperature but of low quality

3. Meltwater

The genesis of taliks is complex, but it can form in any terrain or structural unit. Some taliks (e.g., river taliks) can cover numerous topographical units and structural units, such as mountains, basins, and plains; pass through the distribution area of various rock strata; and contain various groundwater types. Therefore, the groundwater types in a talik cannot be classified with the usual method. Table 2.6 classifies meltwater on the basis of the distribution characteristics, burial conditions, and hydraulic properties of groundwater.

2.6 Earthquakes and Active Faults

Characterized by the wide distribution of large active faults, high-magnitude and frequent seismic activity, long surface rupture zones, and large co-seismic displacement, the Qinghai–Tibet Plateau is currently the most intense area of tectonic movement in the mainland of China.

Seismic problems were important in the investigation and design of the Qinghai–Tibet Railway, as earthquake faults cross the line numerous times. The high seismic intensity and the high risk of surface rupture in the plateau strongly affect the selection of local schemes and the design of engineering structures.

2.6.1 Regional Neotectonic Movement

Neotectonic movement refers to the tectonic movement that has occurred since the Late Tertiary; the tectonic movement in the Qinghai–Tibet Plateau in this period has been highly intensive and frequent. Earthquakes are closely associated with such movement.

The neotectonic movement in the Nanshankou to Kunlun Pass section is characterized by intracontinental compressional orogeny and a strong uplift. The main characteristics of this movement are fold uplift, thrust and strong uplift, large horizontal shrinkage and thickening of the crust, intermontane basin expansion, and obvious vertical movement. The plateau gradually formed after the large horizontal shrinkage and thickening of the crust and expansion of the intermontane basin. Strong earthquakes, hydrothermal activity, and Cenozoic magmatism have been common in the key section from Sangshung to Yambajan. The plateau is the most intense area of modern crustal deformation. Along the Qinghai–Tibet Railway, the highest earthquake intensity regions are between Tuoru and Yambajan in the Nyainqentanglha Mountains area.

2.6.2 Basic Seismic Intensity Zoning

According to the Earthquake Engineering Research Center of China Seismological Bureau, the Qinghai–Tibet Railway line passes through areas with high seismic intensity (intensity > 7). Of the total 1142 km of the Qinghai–Tibet Railway line from Golmud to Lhasa, approximately 620 km (54%), 307 km (27%), and 215 km (19%) passes through seismic zones of intensity 7, 8, and 9, respectively (see Table 2.7).

Table 2.7 Basic seismic intensity zoning of the Qinghai–Tibet Railway

No.	Mileage of the section beginning and end	Section	Basic seismic intensity	Length (km)
1	K814+150–DK866+500	Golmud–Ganlong	7	52.35
2	DK866+500–DK1001+750	Ganlong–Budongquan	8	123.00
3	DK1001+750–DK1585+850	Budongquan–Cuona Lake	7	567.65
4	DK1585+850–DK1712+500	Cuona Lake–Tuoru	8	115.00
5	DK1712+500–DK1933+500	Tuoru–Yambajan	9	215.00
6	DK1933+500–DK2005+918	Yambajan–Lhasa	8	69.00

Table 2.8 Major active faults affecting the engineering of the Qinghai–Tibet Railway

No	Fracture	Details of the line—fault intersection
1	Xidatan Concealed Compressive Fracture	
2	Kunlun Mountains Bealock Compressive Shear Faults	Line passes through three compressive fractures
3	Northern Fenghuo Mountain Compressive Fracture	
4	Wuli Fracture Zone	
5	Yanshiping Regional Compressive Shear Faults	Line passes through seven faults
6	Tonghla Mountain Fault Zone	Line passes through six faults
7	Za'gya Zangbo Active Fault Zone	
8	Touerjiu Mountains Fault Zone	Three faults affect the line
9	Amdo Beishan Fault	
10	South Boundary Active Fault in Amdo Basin	
11	Cuona Lake Eastern Coast Fault	
12	Northern Shengeligong Mountain Fracture	
13	Southern Shengeligong Mountain Fracture	
14	Liantong River–Dimaer Fracture	
15	Tuoru Basin Active Fault	
16	Bengcuo Active Fault	
17	Nyainqentanglha Mountain Eastern Marginal Fault	
18	Damxung Basin Northern Marginal Fault	
19	Langguo–Sangqu Fault	
20	Eastern Boundary fault of Damxung–Yambajan Graben	

2.6.3 Distribution Characteristics of Active Faults

The main structural fault line affecting the Qinghai–Tibet Railway trends nearly EW. The railway line runs NS and passes through the following mountain ranges: (north to south) Kunlun Mountains, Hoh Xil Mountains, Fenghuo Mountain, Kaixinling, Tonglha Mountains, Touerjiu Mountain, Sangxiongling, Jiuzina, and Yangbaling. The line intersects the main structural line at a large angle. Table 2.8 lists the main active faults affecting the railway line.

2.7 Distribution of Permafrost Along the Line

Permafrost is one of the major problems that was encountered in the construction of the Qinghai–Tibet Railway. Permafrost is widely distributed in the Qinghai–Tibet Plateau and is highly sensitive to the environmental conditions, especially temperature. The main railway engineering concerns in the permafrost region are

thawing settlement of the permafrost subgrade, cutting slope collapse and mudflow, tunnel heaving and thawing cracking, icing inside the tunnel, frost heaving and thawing settlement of bridge and culvert foundation, erosion of the concrete surface. Usually, Railways passing through permafrost have a high disease rate after construction, both in China and worldwide. Therefore, solving these problems is key to the success of the Qinghai–Tibet Railway.

2.7.1 Basic Distribution Characteristics

The Qinghai–Tibet Plateau is located in a low latitude area. In contrast to permafrost in high-latitude areas, permafrost here has poor thermal stability, wide distribution of high temperature and high ice content permafrost, and high sensitivity to climate change.

The development and distribution of permafrost along the Qinghai–Tibet Railway is influenced by three directional zonalities: vertical zonality, caused by the altitudinal variation of heat and moisture; latitudinal zonality, caused by latitudinal (north–south) heat difference; and precipitation zonality, which varies with distance from the ocean and with the characteristics of atmospheric circulation. For every 100 m increase in altitude, the annual average temperature decreases by 0.5–0.6 °C and the thickness of the frozen soil increases by approximately 20 m. Similarly, for every 1° southward change in latitude, the altitude increases by 100–130 m, and the lower boundary elevation of the permafrost changes as well.

Permafrost in the plateau is a product of geological development; its occurrence, development, distribution, and evolution is influenced by many geological and geographical factors, such as geological structure, geomorphology, lithology, surface water, groundwater, vegetation, and snowfall, as well as climatic fluctuation over time. The climatic conditions of the plateau—for example, high altitude (approximately 960 km of the plateau is at >4000 m elevation), low pressure (544–600 mb), cold climate (annual average temperature = – 8.5 to –2 °C), long freezing period (permafrost is fully frozen for >7 months/year and frozen during nighttime in the warm season), low annual average temperature of frozen soil (–5 to 0 °C), thin snow, and short preservation time—are the factor that most strongly influences the development and persistence of permafrost. Because of the low latitude, high altitude, and thin snow covering, solar radiation on the plateau is strong.

The annual average temperature in the southern boundary of the Qinghai–Tibet Railway is –3 to –2 °C, which is 1–2 °C lower than that of the southern boundary of the permafrost regions in high-latitude regions. A 120–160-m-long area in the plateau has an annual average temperature of –5 °C. In some regions, the heat flow is high, and thaw areas often form along the structural geotherm. The thick ice layer is mostly distributed in the high moisture-content clay area, and more than 80% of such layers are up to 5 m thick. Typically, atop the ice layer lies a natural upper limit of permafrost. Because of the shallow burial depth, the top surface is easily

affected by variations in the surface conditions and climate, resulting in the frequent development of thaw slumping, thaw lakes and ponds, ice cones, and hummocks.

2.7.2 Distribution of Permafrost Along the Line

Exactly 546.43 km of the Qinghai–Tibet Railway crosses the permafrost zone, with the northern boundary in the Xidatan (DK957+640, altitude = 4350 m, and annual average temperature = -3.6°C) and the southern boundary in Amdo Valley (DK1513+770, altitude 4780 m, and annual average temperature = -2.9°C). Taliks are distributed within these boundaries.

The permafrost regions of the Qinghai–Tibet Railway can be divided into 15 units. A comprehensive evaluation of the engineering geological conditions of each unit is as follows:

1. Xidatan Structural Valley (DK957+640–DK973+700)

In the Xidatan Structural Valley, the Qinghai–Tibet Railway line enters the permafrost region at DK957+640 and passes through the border zone of permafrost and nonpermafrost regions. Four sections totaling 8.518 km, namely DK957+640–DK960+260, DK964+500–DK968+190, DK969+650–DK971+940, and DK972+550–DK973+700, are the permafrost regions and account for 53.5% of the railway mileage in this unit. The remaining sections are nonpermafrost regions or thaw areas.

The main lithology in this unit is alluvial pebble soil and thick pellet soil. The upper limit of permafrost is generally 2.8–3.5 m, the annual average ground temperature of frozen soil is more than -0.5°C , and the permafrost layer is 5–20 m thick. Ice-rich and ice-saturated frozen soils are present in two segments, DK965+410–DK965+740 and DK972+640–DK973+700. Permafrost with high ice content is 1.39 km long (16.3%). Overall, the engineering geological conditions in this unit are favorable, with subgrade being the major engineering structure.

2. Kunlun medium-high mountain area (DK973+700–DK1005+500)

In this unit, the line passes from Luanshi Ditch in Kunlun medium-high mountain area (DK973+700) to Budongquan, crossing Kunlun Mountains Bealock at DK983+600 and Budongquan Valley south of the Kunlun Mountains. A 0.93-km long (2.9% of the line in this unit) talik is present between DK1004+570 and DK1005+500, and the rest of the line passes through 60–120-m-thick permafrost with a 1.5–2.5 m natural permafrost table.

Two sections, DK997+300–DK1002+600 and DK1004+000–DK1004+570, are high-temperature zones of length 5.87 km (12.4%); the remaining 25 km (78.6%) passes through low-temperature zones. Frozen soil with high ice content is distributed mainly along beach land and slopes along 1.39 km of the line (56.1%).

The main lithology in Kunlun Mountain area is weathered broken slate and schist; fine granular soil, such as silt and powder clay in Kunlun Mountain Bealock Basin, and spall soil in Budongquan Valley and beach land. Unfavorable geological phenomena such as thaw slumping, ice cones, and frost mounds are common in the permafrost regions. The railway line passes through seven thaw slumping areas. Overall, the engineering geological conditions in this unit are poor, and filling is the major engineering measure.

3. Chumar River high plain (DK1005+500–DK1072+500)

In this unit, the railway line crosses Qingshui River, Baladacai Meander, and Chumar River. The lithology along the line is fine granular soil such as silt soil, powder clay, and fine sand. A 2.5-km long (3.7% of the line length in this unit) talik is present between DK1072+000 and DK1072+500, accounting for 3.7%. The rest of the line passes through 15–40-m-thick permafrost with a 2.0–5.0 m natural permafrost table.

The line spans 34.9 km (80.5%) and 29.6 km (44.2%) in high- and low-temperature regions, respectively. Frozen soil with high and low ice content is present along 53.93 km (80.5%) and 13.07 km (19.5%) of the line, respectively. No clear pattern is evident in the distribution of high ice content permafrost.

Thaw lakes and ponds, most of which are seasonal, are spread over the plain, and the major engineering measures applied in this unit are embankments and culverts. The ground temperature of the frozen soil here is high, and ice-rich permafrost is widely distributed. With harmful frozen-soil phenomena prevalent, the local engineering geological conditions are adverse.

4. Hoh Xil Mountains (DK1072+500–DK1124+500)

In Hoh Xil Mountain area, the line is mainly distributed over low mountains and hills, with permafrost present throughout. Thaw areas totaling 0.107 km (0.2% of the line length in this unit) are distributed between DK1083+108 and DK1083+215. The rest of the line passes over 30–100-m-thick permafrost with a natural permafrost table of 2.0–3.0 m.

The line passes 42.876 km (81.8%) and 9.41 km (18%) over low- and high-temperature regions, respectively. Ice-rich permafrost (38.775 km; 74%) is the dominant type, with frozen soil with low ice content accounting for only 13.618 km of the line (26%).

The upper section of the ground on which the line passes is mainly fine sand, silt, and other fine granular soil, the a weathered layer of mudstone and marl buried beneath. Because of harmful cryogenic phenomena, thaw lakes or ponds and frozen-soil wetlands are present in this unit. The line uses subgrades to pass through these regions. Nevertheless, annual average ground temperature here is low and the engineering geological conditions average.

5. Beilu River Basin (DK1124+500–DK1145+500)

In Beilu River Basin, the line mainly passes through Xiushui River and the floodplains and terraces of Beilu River. Permafrost is present throughout. A 0.09-km-long talik area (0.4% of the line length in this unit) is present between DK1124+800 and DK1124+910. Accounting for of the whole segment, the length of the talik region is. The rest of the line passes over 10–50-m-thick permafrost with a natural permafrost table of 2.0–3.0 m.

The line passes 15.9 km (75.7%) and 5.1 km (24.3%) over high- and low-temperature regions, respectively. Frozen soil with low ice content is common (13.974 km; 66.5%), and the ice-rich permafrost is mostly located in the Beilu River test Sect. (6.936 km; 33.0%).

Lithology along the line is mainly fine sand, silt, and powder clay, and the overall engineering geological condition is poor.

6. Fenghuo Mountain area (DK1145+500–DK1165+500)

Permafrost is present throughout Fenghuo Mountain area, except for the talik area between DK1149+300 and DK1149+800 (0.5 km long; 2.5% of the line length in this unit); the rest of the regions are mostly permafrost of thickness 50–120 m with a 1.0–2.5 m natural permafrost table.

The line passes 15.3 km (76.5%) and 4.2 km (21%) over low- and high-temperature regions, respectively. Frozen soil with low ice content is the main type (11.49 km; 57.5%), but ice-rich permafrost is mainly distributed in the low hills and depressions (8.01 km; 42%).

The main lithology in the northern and southern Fenghuo Mountain area is powder clay and alluvial spall soil, and interbeds of sandstone and mudstone in the mountain area; the weathered layer is 15–20 m thick. Frozen-soil wetlands are distributed in low hills, over which the line passes through using fills. The slope area over which the line passes is long and is influenced by many unpredictable factors. Hence, ensuring safety was of prime importance during railway construction.

7. Chiqu Valley (DK1165+500–DK1193+200)

In Chiqu Valley, except for the 0.79-km-long (2.9% of the line length in this unit) talik between DK1165+380 and DK1187+170, the railway lines passes through mostly permafrost of thickness 10–50 m with a 2.0–4.0 m natural permafrost table.

The line passes 20 km (72.2%) and 6.91 km (24.9%) over high- and low-temperature regions, respectively. Frozen soil with low ice content is the main type (15.803 km; 57.1%), and ice-rich permafrost present along 11.07 km (40.1%) of the line.

Lithology along the line is mainly brecciated soil and gravelly soil, along with powder clay and fine sandstone in some areas. Few harmful frozen-soil phenomena are present here. The majority of this unit is unstable and has high ground temperatures; the overall engineering geological conditions are average.

8. Wuli Basin (DK1193+200–DK1202+500)

All of Wuli Basin is covered in 50–120-m-thick permafrost with a natural permafrost table of 1.0–2.5 m; no taliks are present in this unstable, high-temperature region, whose annual average ground temperature exceeds -0.5°C . Ice-rich permafrost is the main type of frozen soil here (5.395 km long; 58% of the line length in this unit), and 3.905 km (42%) of the line in this section is over frozen soil with low ice content.

In this basin, the line passes over fine granular soil such as powder clay and fine sandstone. Thaw lakes and ponds and frozen-soil wetlands are major harmful cryogenic phenomena here, and the engineering geological conditions are therefore adverse.

9. Wuli Mountain (DK1202+500–DK1217+700)

Taliks dominate the Wuli Mountain area, accounting for 13.513 km of the line (89% of the line length in this unit). Permafrost of thickness 5–20 m with a 2.0–3.0 m natural permafrost table accounts for 1.687 km (11%). The main type of permafrost in this unit is ice-rich frozen soil (1.186 km), as permafrost with low ice content is present for only 0.501 km. The permafrost here is largely unstable and of high temperature.

In this unit, thaw areas are more widely distributed than are permafrost areas, and the overall engineering geological conditions are favorable, except in the permafrost area.

10. Tuotuo River Basin (DK1217+700–DK1245+000)

Islet permafrost and thaw areas (12.223 km, 44.8% of the line length in this unit) are alternately distributed in this Tuotuo River Basin, where permafrost of thickness 5–30 m with a 2.0–4.0 m natural permafrost Table (15.077 km; 55.2%) is mainly distributed in the low-lying valleys of the northern and southern banks of Tuotuo River; taliks are mainly distributed in the foreland pluvial fan and the first and second terraces of the river.

Apart from the segment between DK1241+850 and DK1245+000, the permafrost here is generally unstable and of high temperature. Permafrost with low ice content is dominant, accounting for one-fifth of the line length, whereas ice-rich frozen soil accounts for only a third of the line in this unit (5.411 km).

Cailloutis soil, thick pellet soil, and other coarse-grained soils are widely distributed here. The line passes through sections of freezing and thawing transition several times, which combined with the high annual average ground temperature makes the local engineering geological conditions adverse.

11. Kaixinling Mountain area (DK1245+000–DK1252+800)

Kaixinling Mountain area has an alternating distribution of thaw areas and permafrost of thickness 20–40 m with a natural permafrost table of 1.5–2.5 m; the thaw areas are dominant. Taliks (7.3 km; 93% of the line length in this unit) are

mainly distributed on gentle hills in Kaixinling, whereas permafrost is mainly distributed in the gullies and intermountain depressions.

Permafrost in this region is unstable and of high temperature and is narrowly distributed. The main type of permafrost in this section is frozen soil with low ice content, and the railway line mainly passes over brecciated soil and gravelly soil. The major harmful frozen-soil phenomenon is frozen-soil wetlands, over which the line uses fills and bridges. Overall, the engineering geological conditions here are not too unfavorable.

12. Tongtian River Basin (DK1252+800–DK1282+800)

In Tongtian River Basin, taliks are distributed between DK1280+500 and DK1282+800 for 2.389 km (8.0% of the line length in this unit); permafrost of thickness 20–40 m with a natural permafrost table of 1.5–3.0 m covers the other areas along the line.

In this unit, the line spans 15.8 km (52.7%) and 11.8 km (39.3%) in the high- and low-temperature regions, respectively. The main type of permafrost in this section is ice-rich frozen soil (20.725 km; 69.0%), as frozen soil with low ice content accounts for only 6.886 km (23%) of the line. The line mostly passes through regions with fine granular soil such as powder clay, silt, and fine sand, and thaw lakes and ponds are prevalent. Overall, the engineering geological conditions here are adverse.

13. Buqu Valley (DK1282+800–DK1360+800)

Apart from some taliks distributed between DK1332+600 and DK1360+800 for 36.045 km (46.2% of the line length in this unit), Buqu Valley is covered in permafrost of thickness 5–40 m with a natural permafrost table of depth 2.0–5.0 m between DK1282+800 and DK 1332+600 for 41.955 km (53.8%).

The permafrost area has poor stability and is of high temperature between DK1352+560 and DK1356+530 (3.97 km; 5%). The main type of permafrost in this unit is frozen soil with low ice content (22.093 km; 52.7%), as ice-rich frozen soil accounts for only (19.862 km; 47.3%).

Ice-rich and low ice frozen soils are distributed rather equally in the permafrost region. The line mainly passes through regions with brecciated soil and gravel soil. Overall, the engineering geological conditions here are of average favorability. However, as the line passes sections with freezing and thawing transition several times, the engineering geological conditions can be adverse in such Sects.

14. Wenquan Fault Basin (DK1360+800–DK1394+800)

An alternating distribution of permafrost and thaw areas can be observed in Wenquan Fault Basin. The thaw area contains river taliks and structural taliks for (9.31 km, 27.4% of the line length in this unit), and permafrost of thickness 5–20 m with a natural permafrost table of 2.0–3.0 m accounts for 24.69 km of the line.

This fault basin has poor stability, and the annual average ground temperature of permafrost is high (more than -0.5°C). Ice-rich permafrost is rare (2.26 km;

6.6%), and low ice frozen soil accounts for the majority of the line length (22.43 km long; 66%).

Lithology along the line is mainly thick pellet soil and brecciated soil, and permafrost wetlands are the main harmful cryogenic phenomena. The line uses roadbeds and bridges to pass through these regions. This fault basin area is a high-temperature region, and the freezing and thawing transition sections make the local engineering setting adverse. Nevertheless, the overall engineering geological conditions are of average favorability.

15. Tonglha Mountains and Intermontane Basin (DK1394+800–DK1485+200)

In Tonglha Mountain area (DK1394+800–DK1513+770), the lines pass over regions with alternating permafrost and taliks (3.831 km; 36.4% of the line length in this unit).

Mostly, permafrost is present between DK1405+320 and DK1456+000 in Tonglha Intermontane Basin area, and a few thaw areas are present in the DK1440+800–DK1443+200 and DK1446+500–DK1449+500 sections for 5.4 km (10.7%).

The talik from Za'gya Zangbo to Amdo (DK1456+000–DK1513+770) spans 12.817 km (22.2%), with permafrost of the thickness 10–120 m with a natural permafrost table of 1.5–3.5 m comprising the rest of the line length.

Most regions (~74.7 km; 62.8%) are high-temperature zones (I, II), and the remaining sections (~31.45 km; 25.3%) are low-temperature zones (III, IV).

Overall, compared with permafrost areas in high-latitude regions, permafrost areas of the Qinghai–Tibet Railway can be characterized as long, ice-rich, and of high temperature. The thermal stability of the frozen soil in the Qinghai–Tibet plateau is dependent on the climatic conditions. Overall, the engineering geological and hydrogeology conditions along the line are complex, the frozen-soil environment complicated, and the ecological environment fragile, all of which rendered difficult the construction of the Qinghai–Tibet Railway.

2.7.3 *Types and Distribution of Thaw Areas in Permafrost Regions*

2.7.3.1 *Types of Thaw Areas*

A thaw area (talik) is a geological body containing either normal-temperature water, no water, or liquid water at subzero temperatures. The occurrence, development, and characteristics of thaw areas in permafrost regions are dependent on such factors as climate, geological structure, hydrological factors, and land cover. Depending on the objective, thaw areas can be classified according to various principles and methods. Table 2.9 presents a classification based on thaw-area genesis.

Table 2.9 Talik classification on the basis of genesis

Genetic type	Talik type	Subclassification
Structural	Structural talik	Structural–geothermal talik
		Structural–surface-water talik
Surface-water	Surface-water talik	River talik
		Lake talik
Infiltration and radiation effects	Infiltration–radiation talik	
Artificial function	Artificial talik	

1. Structural talik

Structural talik is of two types: structural–geothermal and structural–groundwater.

Structural–geothermal taliks are created by underground heat sources. Generally, underground hot water (water temperature $> 45^{\circ}$) rises to the surface through the fault structure to form a hot spring, presenting as a geothermal anomaly. The talik area from DK1282+800 to DK1394+800—which is at the intersection of NW- and NNW-trending compressive shear faults and SN-trending tension–torsion fracture in Buqu Valley—is representative of a structural–geothermal talik. Obviously, the temperature around hot springs is high: around the original 103 Road, which is 100 m away from a modern spring, the geothermal temperature is 7.2°C at a depth of 0.5 m, 12.8°C at 2.5 m, and $>50^{\circ}$ at 40–50 m; 900 m from the spring, the geothermal temperature is 1.5°C at a depth of 1 m, 3.5°C at 3 m, and 12°C at 30 m. The talik is 1.5–2.0 km wide in this area. Hot-spring outcrops can be observed along the intersection of these two groups of faults, such as at the original 90 Road, on both sides of the main ridge on Tonglha Mountains, and in the area between the original 115 and 116 Roads; structural–geothermal taliks can be seen in this outcrop area, the size of which is dependent on the spring temperature and the flow volume.

The formation of structural–groundwater taliks is dependent on the thermal influence of groundwater in the active fault zone. In contrast to structural–geothermal taliks, structural–groundwater taliks are characterized by a low groundwater temperature (generally below 10°C), small size, and poor stability. Taliks of this type are mainly distributed in areas such as Budongquan, Erdaogou, and the Original 85 Road.

2. Surface-water thaw area

Surface-water thaw areas can be further categorized as river taliks and lake taliks.

River taliks exhibit a zonal distribution along the river and are confined to regions within the thermal influence of rivers. The width of these taliks depends on the river volume, water temperature, and the relationship between the river and the geological structure. Some penetrating taliks are distributed in Tuotuo River, Tongtian River, Buqu, and other rivers along the railway line.

The presence of ponding or a supply source for lakes leads to the melting of permafrost and the consequent formation of a penetrating or nonpenetrating talik. Lakes formed by the structure usually form large penetrating taliks. Many lakes and ponds of various sizes are present along rivers such as the Qingshui, Qumar, and Beilu. Taliks are often confined within the water area of these lakes and ponds. A penetrating talik may form at the bottom of lakes because of long-term hydrops, whereas a nonpenetrating talik can only develop in lakes with seasonal water accumulation.

3. Infiltration–radiation thaw area

An infiltration–radiation thaw area can form through two mechanisms: through large-scale surface absorption of solar radiation or through infiltration of atmospheric precipitation. In piece permafrost—islet permafrost transition zones, when all other conditions are almost the same, unequal solar radiation is incident on different slope surfaces, which may cause such phenomena as permafrost and talik in the north and south slopes, respectively. Solar radiation incident on the surface is also affected by the lithology and vegetation. Moreover, infiltration–radiation thaw areas can be distributed within the permafrost regions. Many such areas appear in open terraces or gentle watershed areas with relatively high temperature (more than -1°C). These taliks differ from structural–geothermal taliks as the latter are formed because of recent strong tectonic movement and are geothermal anomalies; they also differ from river taliks, which are often subject to the thermal effect of dynamic water. Therefore, these taliks are often ignored by scholars, but they are nevertheless extensively distributed. For example, these infiltration–radiation thaw areas are spread across thousands of kilometers in Buqu Valley and along tens of kilometers of the northern Tuotuo River. These thaw areas, which are usually exposed, are covered by a layer of thick loose sand and gravel and thus have good drainage.

4. Artificial talik

Human economic activities, such as engineering construction, deforestation and reclamation, drainage and dewatering, water storage projects, and brick stacking, have led to the formation of artificial taliks. These activities have shifted the equilibrium state of the frozen-soil layer, causing heat accumulation at the upper limit of the frozen layer, which in turn results in the melting of the frozen soil or the descending of the upper limit. The range of these activities depends on the generated heat and is usually not much different from the place and scope of the human activities.

The forms and consequences of artificial taliks differ by region, and a lack of awareness of these consequences has caused many problems in engineering construction. Under conditions of low temperature and large thickness, large areas of continuous permafrost always develop nonpenetrating artificial taliks, a phenomenon called thaw bowl. In island permafrost regions, the formation of artificial thawing areas (including other types of financial areas) can reduce the area of permafrost islands or even eliminate them completely, extending the range of the taliks.

Table 2.10 Thaw areas of permafrost regions along the Qinghai–Tibet Railway line

No.	Mileage of the section beginning and end	Length (km)	Talik type	Location
1	DK969+540–DK969+580	0.040	Radiation talik	Frozen-soil boundary in Xidatan
2	DK1004+570–DK1005+500	0.930	Structural talik	Budongquan
3	DK1070+000–DK1072+650	2.650	River talik	Chumar River
4	DK1083+108–DK1083+215	0.107		
5	DK1124+820–DK1124+910	0.090	River talik	Beilu River
6	DK1149+300–DK1149+800	0.500		
7	DK1186+380–DK1187+170	0.790	River talik	Chiqu
8	DK1202+583–DK1202+700	0.117	Structural talik	Wuli Mountain area
9	DK1202+745–DK1206+150	3.405	Structural talik	Wuli Mountain area
10	DK1206+220–DK1209+870	3.650		
11	DK1210+495–DK1211+300	0.805		
12	DK1211+840–DK1214+797	2.957		
13	DK1214+868–DK1217+498	2.630		
14	DK1218+080–DK1221+920	3.840	River talik	Togton River
15	DK1229+476–DK1236+380	6.904	Infiltration–radiation talik	
16	DK1238+390–DK1238+450	0.060		
17	DK1245+210–DK1245+320	0.110	Infiltration–radiation talik	Kaixinling Mountain area
18	DK1245+730–DK1245+815	0.085		
19	DK1245+860–DK1245+930	0.070		
20	DK1245+980–DK1253+990	8.010		
21	DK1280+500–DK1282+889	2.389	River talik	Tongtian River
22	DK1309+000–DK1310+580	1.580	River talik	Buqu
23	DK1312+376–DK1313+136	0.760		
24	DK1313+666–DK1317+948	4.282		
25	DK1318+618–DK1319+340	0.722		
26	DK1319+500–DK1322+736	3.236		
27	DK1322+800–DK1322+903	0.103		
28	DK1322+942–DK1322+995	0.053		
29	DK1324+181–DK1324+596	0.415		
30	DK1325+570–DK1326+180	0.610		
31	DK1326+848–DK1327+374	0.526		
32	DK1327+474–DK1337+100	9.626		
33	DK1338+830–DK1341+740	2.910		
34	DK1341+860–DK1343+130	1.270		
35	DK1344+150–DK1345+200	1.050		
36	DK1346+152–DK1348+560	2.408		
37	DK1348+815–DK1349+390	0.575		
38	DK1349+530–DK1350+220	0.690		
39	DK1350+350–DK1351+090	0.740		
40	DK1351+390–DK1352+560	1.170		
41	DK1356+530–DK1356+900	0.370		
42	DK1357+350–DK1359+300	1.950		
43	DK1360+580–DK1360+700	0.120		

(continued)

Table 2.10 (continued)

No.	Mileage of the section beginning and end	Length (km)	Talik type	Location
44	DK1374+530–DK1375+940	1.410	Structural– groundwater talik	Wenquan Fault Basin
45	DK1378+850–DK1379+140	0.290		
46	DK1379+550–DK1379+650	0.100		
47	DK1380+400–DK1380+960	0.560		
48	DK1381+650–DK1382+400	0.750		
49	DK1382+950–DK1383+300	0.350	Structural– groundwater talik	Wenquan Fault Basin
50	DK1384+050–DK1384+200	0.510		
51	DK1384+550–DK1386+180	1.630		
52	DK1390+430–DK1394+500	4.070		
53	DK1394+710–DK1394+960	0.250	River talik Infiltration–radiation talik	Tonglha Mountain Area and Intermontane Basin
54	DK1395+800–DK1395+846	0.046		
55	DK1396+100–DK1396+450	0.350		
56	DK1396+900–DK1396+990	0.090		
57	DK1397+910–DK1397+950	0.040		
58	DK1398+940–DK1400+200	0.260		
59	DK1400+900–DK1401+460	0.560		
60	DK1401+750–DK1402+300	0.550		
61	DK1403+515–DK1403+700	0.185		
62	DK1404+610–DK1404+650	0.040		
63	DK1404+810–DK1405+320	0.510		
64	DK1441+080–DK1441+430	0.350		
65	DK1442+220–DK1442+300	0.080		
66	DK1442+850–DK1442+950	0.100		
67	DK1446+330–DK1448+700	2.370		
68	DK1458+446–DK1458+760	0.314		
69	DK1468+350–DK1469+290	0.940		
70	DK1469+780–DK1472+680	2.900		
71	DK1474+400–DK1477+100	2.700		
72	DK1480+360–DK1482+800	2.440		
73	DK1501+740–DK1502+030	0.290		
74	DK1509+980–DK1510+870	0.890		
75	DK1511+500–DK1511+950	0.450		
	Total	101.68		

In summary, the formation of artificial taliks affects the natural ecological environment and directly brings about grassland degradation, soil erosion, and other types of environmental deterioration. Therefore, while pursuing economic activities and immediate financial interests, we must not ignore the effects of these activities on the environment.

2.7.3.2 Distribution of Thaw Areas

Exactly 546.43 km of the Qinghai–Tibet Railway line is over the permafrost zone, whereas talik areas account for 101.68 km (18.6%). Table 2.10 summarizes the distribution of thaw areas along the line.

2.8 Unfavorable and Unique Geology Along the Line

The regional geological environment along the Qinghai–Tibet Railway is complex and is home to various unfavorable and unique geological phenomena, such as permafrost, geological hazards in active fault zones and slope areas, geothermal, dust storms, and snowdrift.

2.8.1 *Permafrost*

The major engineering geological problems in permafrost areas are frost heave, thaw settlement, and harmful frozen-soil phenomena. The geological conditions of permafrost along the Qinghai–Tibet Railway are complex and lead to various harmful frozen-soil phenomena.

Harmful frozen-soil phenomena, including unfavorable cryogenic phenomena, refer to the formation of medium–small terrain caused by the freezing and thawing of soil. These phenomena, examples of which include ice cones, ice mantle, frost mounds, gelifluction, thaw slumping, thaw lakes and ponds, frost soil swamps, and permafrost wetlands, adversely affects engineering project.

2.8.2 *Geological Hazards in Active Fault Zones*

The quality of fault rocks along both sides of the railway line is poor, with fault cliffs and fault triangular facets often occurring and forming a volley surface. Thus, geological disasters such as landslides and debris flow can be triggered easily along the line. North of the Qinghai–Tibet Plateau permafrost area, fault activities not only lead to roadbed deformation, pavement cracking, and engineering failure but also induce uneven frosting, structural fracture, migrating ice mounds, and other geological disasters.

A strong earthquake can produce remarkable surface ruptures and cause severe road deformation, bridge damage, and ground-surface subsidence as well as induce unfavorable geological phenomena such as sand liquefaction, collapse, and landslides, further aggravating the disastrous effects of the earthquake.

2.8.3 Geological Hazards in Slope Areas

Types of slopes in the Qinghai–Tibet Plateau include natural hillsides (e.g., along rivers, ditches, and reservoir banks) and general artificial slopes, and these slopes are prone to various geological diseases. Major geological hazards along the Qinghai–Tibet Railway line include dangerous rocks, rockfall, landslides, collapse, landslides, and debris flow; in addition, solifluction, thaw slumping, and slope wetlands occur frequently in permafrost slope areas. Some of these phenomena are explained herein

1. A dangerous rock refers to a rock mass or an individual block of rock on steep slopes and having a potential to collapse or fall, and rockfall refers to the phenomenon wherein an individual rock block suddenly falls or rolls down a steep slope under the effect of gravity. Collapse refers to the phenomenon wherein a rock mass suddenly falls down a steep slope under the effect of gravity or other forces (e.g., toppling, caving, and rolling). Slope deformation caused by these movements is also a type of collapse.
2. Because of either geological processes or human activities, a rock or soil mass may suddenly or quickly move entirely or partly down the slope of a weak surface; the resulting topography is referred to as a landslide.
3. Rainfall- or snowmelt-induced Debris flow is common in mountain areas. This phenomenon is a type of flood that carries a large amount of silt, stones, and other loose solid material.
4. Solifluction is the phenomenon wherein the structure of a turf and epipedon soil is damaged because of repeated freezing and thawing, following which the saturated soil slowly creeps down the hillside.
5. Slope wetlands are of two types: frozen-soil and nonfrozen-soil slope wetlands. Wetlands in permafrost slope areas are discussed comprehensively in the Sect. 5.2 of Chap. 5. Wetlands in nonpermafrost slope areas mainly contain cohesive soil. Strong infiltration and poor groundwater runoff in cohesive soil with or without rich humus gradually result in the formation of swamping wetlands.

2.8.4 Geothermal Activity, Sandstorms, and Snowdrifts

The area along the Qinghai–Tibet Railway has abundant geothermal and wind resources; however, it also has some unique and unfavorable geological phenomena such as geothermal activity, aeolian drift, and snowdrift, all of which adversely have affected the construction and maintenance of the railway line

1. Geothermal activities and human exploitation of geothermal resources may change the geological environment and trigger geological hazards, such as collapse and landslide due to the alteration of the structural characteristics of the

geological body, ground subsidence due to water drainage, and soil salinization due to geothermal fluid leaching. Furthermore, geothermal activity can alter the geological environment, either facilitating or hindering landslides, hydrothermal cementations, and soil salinization.

2. Aeolian drift in the area along the Qinghai–Tibet Railway, mainly presenting as severe sand burial and wind erosion of the railway line is a major effect of the characteristics of the plateau, namely strong wind, abundant sand availability, dry and warm climate, rapid population and livestock growth, and growth in the intensity of human and livestock activities.
3. Because of the wide distribution of snow on the plateau, snow damage such as avalanche and snowdrift (snow-bearing wind) is severe; snowdrift in particular adversely affects the Qinghai–Tibet Railway line.

2.9 Summary

Characterized by high elevation, low temperature, hypobaric hypoxia, and continuous permafrost, the Qinghai–Tibet Railway runs through a harsh environment with a fragile ecosystem.

This chapter introduced the geographical conditions along the Qinghai–Tibet Railway, including the local geography, climatic characteristics, soil and vegetation, wildlife, river system, and ecological environment. In particular, the geological environment along the railway line—including the topography, formation lithology, geological structure, hydrogeology, seismic and active faults, permafrost distribution, and geology—was described in detail.

The engineering geological conditions along the line—especially permafrost, earthquake intensity zoning, and geological hazards in slope areas—are complex, which along with the necessity of environment protection strongly influence line selection. In sum, a comprehensive analysis of the various engineering geological conditions along the line is essential for studying the line scheme.

References

1. Agricultural Resources Division Office, Qinghai Province. (1997). *Soil of Qinghai*. China Agriculture Press (in Chinese), Beijing.
2. Cao, D. Y., Lei, Y. D., Deng, X. F., et al. (2007). General engineering geological conditions along the Naij Tal-Tuotuo River section of the Qinghai–Tibet Railway. *Qinghai Environment*, 17(2), 78–80. (in Chinese).
3. Chen, R. H., & Wang, Z. T. (2003). Engineering-geological route selection of the gypsum section from Buqu to Wenquan of the Qinghai–Tibet Railway. *Journal of Glaciology and Geocryology*, 25(1), 14–16. (in Chinese).
4. Chen, M. X., Wang, J. Y., & Deng, X. (1994). *Geothermal resource of China: Forming characteristics and the potential assessment*. Beijing: Science Press. (in Chinese).

5. China Railway First Survey & Design Institute Group Co., Ltd. (1994). *The manual of routes* (2nd ed.). Beijing: China Railway Press. (in Chinese).
6. China Railway First Survey & Design Institute Group Co., Ltd. (2002). *Preliminary design of the Tonglha–Lhasa section of the Qinghai–Tibet Railway (Geology)*. Internal information. (in Chinese).
7. China Stratigraphic Lexicon Editorial Board. (2000). *China stratigraphic lexicon: Quaternary*. Beijing: Geological Publishing House. (in Chinese).
8. Dai, J. X. (1990). *The climate of the Tibetan Plateau*. Beijing: Meteorological Press. (in Chinese).
9. Lanzhou Glacier Frozen Soil Research Institute, Chinese Academy of Sciences. (1983). *Collected papers of Tibet frozen soil research*. Beijing: Science Press. (in Chinese).
10. Li, W. Y. (1988). *Quaternary plants and environment in China*. Beijing: Science Press. (in Chinese).
11. Liang, S. H., Chen, J., Jin, X. M., et al. (2007). Regularity of vegetation coverage changes in the Tibetan Plateau over the last 21 Years. *Advances in Earth Science*, 22(1), 33–40. (in Chinese).
12. Liu, Z. P. (2008). Distribution characteristics of permafrost development along the Qinghai–Tibet Railway. *Railway Investigation and Surveying*, 2, 78–82. (in Chinese).
13. Liu, Z. Q., Xu, X., Pan, G. T., et al. (1990). *Geotecture and evolution of the Tibetan Plateau*. Beijing: Geological Press. (in Chinese).
14. Ma, T., Zhou, J. X., Zhang, X. D., et al. (2007). Preliminary studies on characteristics of vegetation distribution along the Qinghai–Tibet Railway line. *Research of Soil and Water Conservation*, 14(3), 150–154. (in Chinese).
15. Meng, X. L. (2006). Geological prospecting for permafrost engineering in the Qinghai–Tibet Railway. *Railway Investigation and Surveying*, 3, 28–31. (in Chinese).
16. Papers and reports on permafrost in the Qinghai–Tibet Plateau. *Annual Report of State Key Laboratory of Frozen Soil Engineering*. (in Chinese).
17. State Seismological Bureau of China. (1991). *Earthquake intensity zoning map of China (1990)*. Beijing: Earthquake Press. (in Chinese).
18. Sun, Y. F. (2005). Permafrost engineering in the Qinghai–Tibet Railway: Research and practice. *Journal of Glaciology and Geocryology*, 27(2), 153–162. (in Chinese).
19. The China Society on Tibet Plateau. (1995). *Collected papers of seminar on the Tibetan Plateau and global change*. Beijing: Meteorological Press. (in Chinese).
20. The Expert Panels of the Qinghai–Tibet Projects. (1995). *Research on the formation and evolution of environmental changes and ecosystem of the Qinghai–Tibet Plateau*. Beijing: Science Press. (in Chinese).
21. The Glacier Permafrost Research Room, Institute of Geography, Chinese Academy of Sciences. (1965). *Investigation of frozen soil along the Qinghai–Tibet Highway*. Beijing: Science Press. (in Chinese).
22. Tong, C. J. (1996). *Geological evaluation and treatment of frozen soil in permafrost along the Qinghai–Tibet Highway*. Beijing: Science Press. (in Chinese).
23. Wang, Y. D. (2002). Preliminary exploration of geologic route selection in multiyear tundra of Qing–Zang Railway line. *Journal of Railway Engineering Society*, 2, 57–59. (in Chinese).
24. Wang, Z. H. (2006). Active tectonics and its secondary disasters along the Qinghai–Tibet Railway. *Journal of Railway Engineering Society, Supplements*, 1, 264–269. (in Chinese).
25. Wang, Z. H. (2007). Geological environment and disasters along the railway line in the Qinghai–Tibet Plateau. *Earth Science Frontiers*, 14(6), 031–037. (in Chinese).
26. Wang, Q. Q., Qin, N. S., Tang, H. Y., et al. (2007). Study on climate change facts and their characteristics in the Qinghai Plateau in the recent 44 years. *Arid Zone Research*, 24(2), 234–239. (in Chinese).
27. Wei, G. J. (2003). Geological line selection of the Xiaonanchuan–Wangkun unfavorable geological section of the Qinghai–Tibet Railway. *Geotechnical Engineering World*, 6(7), 41–45. (in Chinese).

28. Wu, Z. W., Chen, G. D., et al. (1988). *Roadbed engineering in frozen earth area*. Lanzhou: Lanzhou University Press. (in Chinese).
29. Wu, Z. H., Ye, P. S., Wu, Z. H., et al. (2003). Hazard effects of active faulting along the Golmud-Lhasa Railway across the Tibetan Plateau. *Modern Geological*, 17(1), 1–7. (in Chinese).
30. Wu, Z. H., Hu, D. G., Wu, Z. H., et al. (2006). Migrating pingos and their hazard effects in the vicinity of the railway across the northern Tibetan Plateau. *Geological Bulletin of China*, 25 (1–2), 233–243. (in Chinese).
31. Yang, Y. F., Jiang, H., Niu, F. J., et al. (2007). Space-time variation analyses of air temperature over the Qinghai-Xizang Plateau in warm and cold seasons. *Plateau Meteorology*, 26(3), 496–502. (in Chinese).
32. Ye, D. Z., Gao, Y. X., Shen, Z. B., et al. (1979). *The meteorology of the Qinghai-Tibet Plateau*. Beijing: Science Press. (in Chinese).
33. Yi, M. C., Wu, Z. H., Hu, D. G., et al. (2003). N-S-trending active structures along the Qinghai-Tibet Railway and their influences on railway bed engineering. *Journal of Geomechanics*, 10(3), 343–354. (in Chinese).
34. Yi, Z. M., Zhou, J. X., & Zhang, X. D. (2006). Analysis of hydrologic conditions along the Qinghai-Tibet Railway. *Technology of Soil and Water Conservation*, 4, 14–16. (in Chinese).
35. Yin, A. (2001). Geologic evolution of the Himalayan-Tibetan orogen. *Acta Geophysica Sinci*, 22(3), 193–238. (in Chinese).
36. Zhang, G. X., Wang, S. J., & Zhang, Z. Y. (2000). *China engineering geology*. Beijing: Science Press. (in Chinese).
37. Zhao, J. C., Liu, S. Z., & Ji, S. W. (2001). Engineering-geological problems in railway engineering construction. *The Chinese Journal of Geological Hazard and Control*, 12(1), 7–9. (in Chinese).
38. Zhou, Y. W., et al. (2000). *China frozen soil*. Science Press. (in Chinese).
39. Zhou, J. X., Yi, Z. M., Li, D. X., et al. (2007). Distribution patterns of species diversity of natural vegetation along the Qinghai-Tibet Railway. *Journal of Soil and Water Conservation*, 21(3), 173–187. (in Chinese).

Geological Line Selection for the Qinghai-Tibet Railway
Engineering

Li, J.; Wang, N.; Liu, Z.

2018, XVII, 315 p. 61 illus., 13 illus. in color., Hardcover

ISBN: 978-3-662-55570-5